Remobilisation of the continental lithosphere by a mantle plume: major-, trace-element, and Sr-, Nd-, and Pb-isotope evidence from picritic and tholeiitic lavas of the Noril'sk Dis...

Article *in* Contributions to Mineralogy and Petrology · June 1993

DOI: 10.1007/BF00307754

CITATIONS
336

READS
150

7 authors, including:

C. J. Hawkesworth
University of St Andrews
538 PUBLICATIONS **41,299** CITATIONS
SEE PROFILE

N. S. Gorbachev
Russian Academy of Sciences
69 PUBLICATIONS **1,524** CITATIONS
SEE PROFILE

Contrib Mineral Petrol (1993) 114:171–188

Contributions to Mineralogy and Petrology

Remobilisation of the continental lithosphere by a mantle plume: major-, trace-element, and Sr-, Nd-, and Pb-isotope evidence from picritic and tholeiitic lavas of the Noril'sk District, Siberian Trap, Russia

P.C. Lightfoot[1], C.J. Hawkesworth[2], J. Hergt[2], A.J. Naldrett[3], N.S. Gorbachev[4], V.A. Fedorenko[5], and W. Doherty[6]

[1] Precambrian Geoscience Section, Ontario Geological Survey, Willet G. Miller Centre, Laurentian University Campus, 933 Ramsey Lake Road, Sudbury, Ontario, P3E 6B5, Canada
[2] Department of Earth Sciences, The Open University, Milton Keynes, MK7 6AA, UK
[3] Department of Earth Sciences, The University of Toronto, Toronto, Ontario M5S 1A1, Canada
[4] Institute of Experimental Mineralogy, Russian Academy of Sciences, 142432 Chernogolovka, Moscow District, Russia
[5] Central Geological Institute for Exploration and Research (TsNIGRI), Russian Ministry of Geology, Moscow, Russia
[6] Geological Survey of Canada, 601 Booth St., Ottawa, Ontario, K1A OE8, Canada

Received May 18, 1992/Accepted November 3, 1992

Abstract. The Late Permian to Early Triassic Siberian Traps have been sampled by drill core (core SG-9) and from surface exposure (section 1F) in the Noril'sk region of the Siberian Platform, Russia. Combined major, trace element, and Nd-, Sr-, and Pb-isotope data on selected samples through the Siberian Trap, offer new chemostratigraphic criteria for the identification and characterisation of two fundamentally different magma types and 9 of the 11 formations of lava developed near Noril'sk. A Lower Sequence of sub-alkalic basalts, tholeiites, and picritic basalts (upwards these are the Ivakinsky, Syverminsky, and Gudchichinsky formations) are overlain by an Upper Sequence of picritic basalts and tholeiites interbedded with tuffs (upwards, these are the Khakanchansky, Tuklonsky, Nadezhdinsky, Morongovsky, Mokulaevsky and Kharayelakhsky formations). The Gudchichinsky and Tuklonsky formations contain both picritic and tholeiitic lavas. The Tuklonsky formation tholeiites and picrites have moderate Gd/Yb (1.6–1.8), low TiO_2 (0.45–0.95 wt%), a significant negative Ta and Nb anomaly (Nb/La = 0.42–0.57) and unradiogenic Nd (ε_{Nd}^{CHUR} = 0 to −4.6). In contrast, both the Gudchichinsky formation tholeiites and picrites have high Gd/Yb (2.3–3.1), and TiO_2 (1.2–2.3 wt%), no significant Nb or Ta anomaly (Nb/La = 0.8–1.1), and radiogenic Nd (ε_{Nd}^{CHUR} = 3.7 to 7.3). The low-Ti and Nb/La, high La/Sm, and unradiogenic Nd-isotope signatures of the picritic Tuklonsky formation lavas and the tholeiitic lavas of the Upper Sequence are characteristic of magmas strongly influenced by material from the continental lithosphere, whereas the high-Ti and Nb/La, low La/Sm and radiogenic Nd-isotope signatures of the Lower Sequence are more comparable to deeper asthenospheric mantle-plume generated lavas similar to oceanic island basalts. The lavas overlying the Tuklonsky formation have mg-numbers of 0.63 to 0.68, and are more evolved than the Tuklonsky (Mg-number < 0.62) and have more radiogenic ε_{Nd}^{CHUR} (Tuklonsky: −0.03 to −4.66; Mokulaevsky: +0.60 to +1.61), but have many of the incompatible trace element features of the Tuklonsky type magma. These lavas show a progressive upwards decline in SiO_2 (55–49 wt%), La/Sm (4.6–2.0), and ε_{Sr}^{UR} (+67 to +13) which has previously been attributed to a decrease in the proportion of crustal material contributed to the magma. This paper explores an alternative model where a component of the crustal contribution might be derived from within an ancient region of the mantle lithosphere as recycled sediment rather than from the overlying continental crust.

Correspondence to: P. Lightfoot

Introduction

Continental Flood Basalt (CFB) provinces represent major magmatic events in which large volumes of magma are generated over relatively short periods of time. In the case of the Siberian Trap, it is believed that the original volume of magma exceeded $1.5*10^6$ km^3 (Zolotukhin and Al'mukhamedov 1988), and that these lavas were erupted over a period of as little as 1–2Ma (Renne and Basu 1991) at the Permotriassic boundary. Major controversies remain over how they were generated, and the extent to which they sampled the asthenospheric mantle, or a distinctive, if not unique reservoir in the continental mantle lithosphere. In this paper we present new major and trace element data, and Sr-, Nd-, and Pb-isotope data from two sequences of stratigraphically controlled lavas from the Noril'sk District of the Siberian Platform which lies close to the Permotriassic site of the Jan Mayen hot spot (Morgan 1981). We address the following agenda:

(1) The chemostratigraphy for the Noril'sk lavas.

(2) The compositional diversity within and between lava formations, and more specifically, the origin of two formations (the Gudchichinsky and Tuklonsky) which include both tholeiitic and picritic lavas with high- and low-TiO_2.

(3) The relative contributions of asthenospheric and lithospheric mantle to CFB magmatism in the Noril'sk District, Siberia.

(4) The relative contributions of crust and mantle, and the process by which mantle derived magmas inherit a component of continental crust.

Specifically, the results are used to show that both picritic and tholeiitic magmas inherit the signatures of at least two different sources. The Lower Sequence is dominantly derived from plume related material in the asthenospheric mantle, perhaps linked to a mantle plume concentrated northwest of the Noril'sk Region at the junction of the Yenisei-Khatanga basin with the west Siberian lowlands. In contrast, the Upper Sequence is dominated by contributions from ancient continental lithospheric mantle which contains a component of recycled crustal material (Hergt et al. 1991; Ellam and Cox 1991). We then speculate on the role of the mantle plume originating beneath the lithospheric mantle in the generation of the Siberian Trap, and the process by which the stagnant mechanical boundary layer of the continental mantle lithosphere might contribute a chemical signature to the lavas.

General geology

The Siberian basalts analysed are from the Noril'sk district at the northwestern margin of the Siberian Platform (Fig. 1). The basalts were erupted onto a sequence of Upper Proterozoic to Upper Permian sedimentary rocks. The sediments and basalts were subsequently affected by a later series of SW-NE and SSE-NNW faults (Fig. 1). A drill core (SG-9) and a surface section (1F) provides a nearly continuous record through the basalts (cf. Lightfoot et al. 1990b). On the basis of field and drill core together with petrographic and geochemical features (Fedorenko 1979, 1981, 1991) and trace element geochemical data (Lightfoot et al. 1990b; Naldrett et al. 1992; Lightfoot, unpublished data), these Permotriassic lavas have been subdivided into eleven basalt suites which are developed in the same relative sequence, are confined to different depth intervals, and may therefore be regarded as stratigraphic units of formations (Cox and Hawkesworth, 1984; Table 1). The lower three formations (Lower Sequence) include sub-alkalic basalts, tholeiites and locally picritic basalts of the Ivakinsky, Syverminsky and Gudchichinsky formations (Table 1). The Upper Sequence consists of eight formations of tuffs, tholeiitic and locally picritic basalts (the Khakanchansky, Tuklonsky, Nadezhdinsky, Morongovsky, Mokulaevsky, Kharayelakhsky, Kumginsky, and Samoedsky formations as shown in Table 1). Picritic and tholeiitic basalts are developed in the Gudchichinsky and Tuklonsky; the picritic flows are allocated to the Tuklonsky and Gudchichinsky picritic basalt units (TPBU and GPBU, respectively).

The emplacement of Lower Sequence lavas appears to have followed the lineaments defined by or proximal to the Noril'sk-Kharayelakh and North Kharayelakhsky faults (Fig. 1; Fedorenko, 1979, 1991; Lightfoot et al. 1990b, Naldrett et al. 1992). Gudchichinsky lavas primarily occur in basinal depressions along the line of the Yenisey-Khatanga trough, and the eruption of Tuklonsky lavas was centred to the east along the Imangdinsky fault to the east (Fig. 1; Fedorenko, 1979, 1991; Lightfoot et al. 1990b). A return to the Noril'sk-Kharayelakh fault heralded the eruption of Nadezhdinsky lavas, but the overlying Morongovsky and Mokulaevsky lavas then thicken to the east, marking the migration of the volcanic edifice to the east again (Fedorenko 1979, 1991; Lightfoot et al. 1990b; Naldrett et al. 1992).

The Noril'sk basalts represent a very small percentage of the entire Siberian Trap, but show some of the greatest petrological and geochemical variety, and are important in the context of associated Cu, Ni, and platinum group element mineralisation in associated intrusions. Sharma et al. (1991) provide geochemical data for the Putorana basalts to the southeast.

The basalt sequences in core SG-9 and section 1F are different in flow thickness, formation thickness, and petrography. In core SG-9, there is only one horizon of picritic lavas, whereas in section 1F there are two well developed picritic lava horizons. Section 1F consists of more than 45 recognisable flow units (Lightfoot et al. in prep.) and four well developed tuff horizons in a 850 m surface section. In core SG-9, there are at least 72 discrete flow units or packages of flows forming compound-type flow units (cf. Lightfoot 1985) in a 2200 m section. There are 17 tuff horizons preserved in core SG-9. Tuffs dominate in the Upper Sequence and are more sparse in the Lower Sequence. This presumably reflects the greater importance of explosive volcanic activity in the eruption of the Upper Sequence.

The field and drill core features of importance include the thick Khakanchansky tuff which separates the Lower from the Upper Sequence in both drill core SG-9 and section 1F, and this is recognised throughout the Noril'sk region (Federonko 1979, 1991; Lightfoot et al. 1990b). The picritic flows of the Gudchichinsky and Tuklonsky formations are also useful marker horizons, and importantly data for core SG-9 and section 1F confirm that the Tuklonsky picrites are laterally discontinuous between these two locations, whereas the picritic lavas of the Gudchichinsky are developed in both locations. In both core SG-9 and section 1F, Syverminsky and Gudchichinsky tholeiites constitute well developed packages of flows comparable to the compound type flow units described elsewhere (e.g. the Deccan Trap).

The detailed petrography of the low-Mg basalts in section 1F is given in Lightfoot et al. (in prep.), and comparable data are available for core SG-9 (Lightfoot et al. in prep.). The flows of the Ivakinsky consist of Ti-augitic basalts in both core SG-9 and section 1F (referred to as the Iv_2 unit). These are overlain by labradoritic and two-plagioclase basalts (in core SG-9), and andesine basalts (in section 1F). Lower Ivakinsky trachybasalts (Iv_1) are absent in both the core and section. The intrusions of trachydolerites are believed to be comagmatic to Iv_1 lavas and are represented in core SG-9 (sample 2200). The Syverminsky consists of unsubdivided tholeiitic basalts in both core SG-9 and section 1F. The Gudchichinsky basalts comprise a basal glomeroporphyritic flow overlain by porphyritic and poikilophitic basalts (grouped in unit Gd_1), followed by tholeiites and picritic basalts of unit Gd_2 (the picrites are grouped in the Gudchichinsky picritic basalt unit, GPBU). The Khakanchansky consists of tuffs in the Noril'sk region and it has not been subdivided. Tuklonsky formation lavas in section 1F consist of a lower sequence of dominantly poikilophitic basalts (Tk_1), overlain by a compound flow sequence of picritic basalts (grouped in the Tuklonsky picritic basalt unit, TPBU). Nadezhdinsky lavas in core SG-9 and section 1F include porphyritic and tholeiitic basalts (Nd_1), porphyritic basalts and tuffs (Nd_2), and glomeroporphyritic basalts (Nd_3). Nd_3 lavas have been allocated to the Morongovsky formation by Naldrett et al. (1992). Morongovsky lavas include aphyric, poikilophitic, and porphyritic flows in places separated by tuffs in section SG9, and are not known at the top of section 1F. The overlying Mokulaevsky includes porphyritic, poikilophitic, aphyric, and glomeroporphyritic flows and tuffs in core SG-9. One sample of Kharayelakhsky lava is preserved at the top of core SG-9 (sample no. 85.6). Kumginsky and Samoedsky lavas are not developed in these sections but are currently being investigated in two other sections (15F and 16F). The Kharayelakhsky and Samoedsky are known to consist of complex intercalations of porphyritic, poikilophytic, aphyric, glomeroporphyritic and aphyric basalts; the

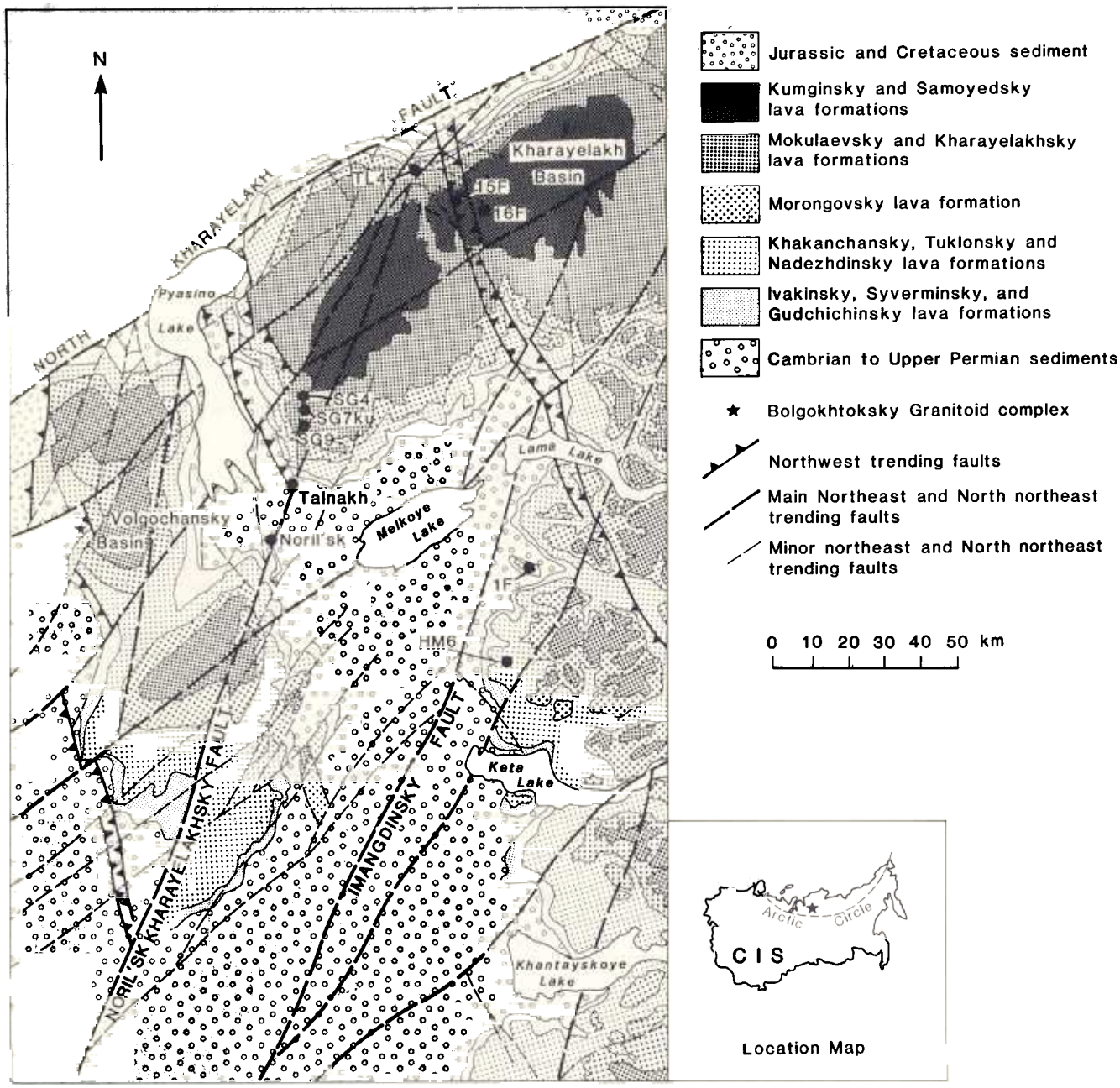

Fig. 1. Map showing the distribution of basalts in the Noril'sk Region and the location of the sampled core and sections

Kumginsky is known to be dominated by glomeroporphyritic basalts.

The petrography of the tholeiitic basalts includes abundant plagioclase phenocrysts with lesser augite, and pseudomorphed olivine grains. The groundmass contains glass, anhedral grains of magnetite, and ilmenite needles. Picritic basalts tend to be more altered with pseudomorphed olivine in a groundmass of augite pyroxene, plagioclase and opaques.

The petrographic data suggest that correlations can be made throughout the Noril'sk district between some tuff horizons and distinctive packages of porphyritic, glomeroporphyritic and tholeiitic basalts. In detail, however, these correlations can only be confirmed with detailed geochemical data.

Sampling, sample preparation, analytical methods, and results

Representative samples weighing 100–500 g were collected from 1" drill core and surface exposure by one of us (V.A.F.). The samples were crushed using a steel-plate jaw crusher and coarser amygdaloidal fragments were removed. The samples were then ground in 99.8% pure alumina planetary mills. These mills are known to introduce a maximum of 0.25% Al_2O_3 during a routine sample preparation of this size (Lightfoot et al. 1990b). Major and trace element analytical data were determined in the Geoscience Laboratories of the Ontario Geological Survey following the published analytical methodologies (Ontario Geological Survey 1990). The

Table 1. Stratigraphy of the Siberian Trap lavas at Noril'sk: variations in thickness of formations and units, and in petrography

Formation	Group	Range of Thickness (m)	Lithology	Developed in Core SG-9	Section 1F
Samoedsky	T_2sm_3	> 200	Poikilophitic, aphyric, and glomeroporphyritic basalt.		
	T_2sm_2	230–280	Aphyric, poikilophitic, and porphyritic, gomeroporphyritic basalt, and tuffs.		
	T_2sm_1	140–180	Aphyric and porphyritic basalts with tuff lenses.		
Kumginsky	T_2km	160–210	Glomeroporphyritic basalts with tuff horizon.		
Kharayelakhsky	T_2hr_4	95–215	Poikilophitic, porphyritic, and aphyric basalts, andesine basalts with tuffs.		
	T_2hr_3	205–365	Poikilophitic, porphyritic, and aphyric basalts with some tuffs	– 120	
	T_2hr_2	15–210	Glomeroporphyritic basalt.		
	T_2hr_1	60–105	Porphyritic, aphyric and poikilophitic basalts with thick tuffs at base.		
Mokulaevsky	T_1mk_4	40–165	Aphyric, poikilophitic and porphyritic basalts and tuffs.		
	T_1mk_3	140–265	Poikilophitic, aphyric and porphyritic basalts.	250	
	T_1mk_2	40–290	Glomeroporphyritic basalts with some porphyritic, aphyric, and poikilophitic basalts.	65	
	T_1mk_1	35–275	Porphyritic and aphyric basalts.	– 275	
	T_1mr_2	175–640	Aphyric and poikilophitic basalts; rare porphyritic and glomeroporphyritic basalts. Thick tuffs. Ankaramites to NE, trachybasalts to SE.	– 280	
	T_1mr_1	45–150	Aphyric, poikilophitic, and porphyritic basalts; tuffs.	– 90	
Nadezhdinsky	T_1nd_3	25–150	Glomerophyritic basalts (one flow porphyritic near base); tuffs.	– 140	– 40
	T_1nd_2	75–260	Porphyritic, glomeroporphyritic basalts, tuff horizon at base	– 170	– 110
	T_1nd_1	50–260	Porphyritic and tholeiitic basalts.	– 230	– 160
Tuklonsky	T_1tk (TPBU)	0–220	Poikilophitic and picritic basalts; tuffs.		– 170
Khakanchansky	T_1hk	10–260	Tuffs separated by poikilophitic basalts in place.	– 20	– 20
Gudchichinsky	T_1gd_2 (GPBU)	0–190	Picritic basalts, picrite-like and olivine phyric tholeiites.	– 110	– 15
	T_1gd_1	0–160	Poikilophitic, porphyritic, and glomeroporphyritic basalts; tuffs.	– 50	– 30
Syverminsky	T_1sv	0–195	Tholeiitic basalts.	– 130	– 160
Ivakinsky	P_2iv_3	0–135	Subalkaline, labradoritic, two-plagioclase andesine basalts and tuffs.	– 90	– 40
		0–100	Subalkaline, Ti-augitic and poikilophitic basalts, tuffs and tuff breccias.	30	30
	P_2iv_1	0–240	Alkaline trachybasalts, tuffs and tuff breccias.		

major element oxides were determined by wavelength dispersive X-ray fluorescence; the rare-earth elements, Y, Zr, Nb, Rb, Sr, Cs, Th, U, Ta, and Hf were determined by inductively coupled plasma mass spectrometry using the Ru-Re internal standardisation scheme on solutions stabilised in the presence of HF (Doherty 1989; Doherty et al. 1990); Ni, Cu, Co, Sc, V, and Zn were determined by inductively coupled plasma emission spectrometry; Ba and Cr were determined by flame atomic absorption. In Table 2, selected major element oxides are re-calculated to 100% free of loss-on-ignition (LOI). Three of the larger (> 400 g) samples were split in half, and prepared in duplicate. No significant difference in the analysis of the two portions resulted (Lightfoot et al. in prep.), suggesting that the sampling, preparation and analytical protocols were not biased by inadequate sampling or sample preparation. Quality control measures included the analysis of the in-house Keweenawan basalt standard MRB-29 (Lightfoot et al. 1991) as an unknown (a blind standard) with the samples, samples which were treated as blind duplicates, and the routine determination of international standards such as BHVO-1. The analyses of MRB-29 indicate that precision over the period of analytical work was 5% RSD, or better. Duplicate determinations of analytes in the same samples verified a worst case 5% RSD precision. Analytical data for BHVO-1 verify the accuracy to be 5% RSD or better. The instrumental methods were able to determine all of the analytes in all samples at levels well above the analytical six sigma determination limit (Potts 1987). An analytical data bank for 97 volcanic samples forms the basis of the present study (Table 2 shows a subset of these analyses). These consist of 45 new whole rock analyses of samples from the study of section IF (Table 2 and unpublished data), 44 whole rock analyses published by Lightfoot et al. (1990b) for core SG-9, and 8 analyses of Ivakinsky, Syverminsky, and Gudchichinsky basalt from other cores in the Noril'sk district (unpublished data).

Sr-, Nd-, and Pb-isotope determinations were made at the Open University Isotope Facility. Separations followed conventional anion and cation exchange methods; analyses were acquired using a Finnigan Matt magnetic sector thermal ionisation instrument and corrected for mass fractionation. Data for reference standards and control materials are given in Table 3.

Chemostratigraphy

Figure 2a shows selected major and trace element data (mg-number, TiO_2, La/Sm and Gd/Yb) and Sr- and Nd-isotope data from core SG-9; major and trace element

Table 2. Major and trace element compositional data for selected samples from section 1F, Imangdinksy Districts, Russia

Depth (m)	Core/ Section (Sample no.)	Formation	mg -number[a]	SiO_2	TiO_2	Al_2O_3	Fe_2O_3	MgO	MnO	CaO	Na_2O	K_2O	P_2O_5	L.O.I.[a]
128	1F(2)	Iv	0.363	52.8	2.31	14.6	13.2	3.24	0.17	6.99	3.46	2.38	0.84	1.7
197	1F(7)	Sv	0.571	54.7	1.57	14.8	10.7	6.10	0.16	6.26	3.40	2.13	0.23	2.8
249	1F(11)	Sv	0.581	53.5	1.63	15.4	10.7	6.36	0.14	7.61	2.45	1.93	0.26	5.0
308	1F(16)	Sv	0.550	51.2	1.65	15.3	11.7	6.15	0.14	8.71	4.06	0.76	0.29	3.9
329	1F(18)	GPBU	0.707	46.4	1.61	8.63	16.7	17.3	0.23	8.10	0.89	0.03	0.15	8.1
377	1F(22)	Tk1	0.657	49.7	0.84	15.4	11.1	9.14	0.18	10.4	2.81	0.37	0.08	3.0
454	1F(25)	Tk1	0.652	49.5	0.90	15.9	10.6	8.54	0.15	12.4	1.81	0.13	0.08	4.7
484	1F(28)	Tk1	0.644	49.6	0.91	16.1	10.9	8.48	0.18	11.6	1.59	0.51	0.08	4.0
512	1F(30)	TPBU	0.754	47.8	0.71	12.0	12.5	16.5	0.18	9.22	0.77	0.31	0.05	5.9
525	1F(33)	TPBU	0.762	46.8	0.45	12.7	11.5	15.8	0.18	11.4	0.91	0.19	0.05	4.7
565	1F(34)	Nd1	0.615	52.8	0.88	15.5	9.90	6.79	0.16	10.8	2.08	1.00	0.11	2.1
666	1F(38)	Nd1	0.595	51.8	1.00	15.7	10.6	6.69	0.20	9.23	1.93	2.67	0.12	3.6
751	1F(41)	Nd2	0.554	52.9	1.06	15.5	10.9	5.82	0.16	10.1	2.53	0.97	0.13	1.6
820	1F(44)	Nd3	0.576	50.7	1.18	15.2	12.0	7.00	0.19	11.1	1.78	0.76	0.15	
Obs MRB-29[d]				49.5	1.91	12.56	13.46	6.09	0.18	9.25	2.39	0.71	0.25	2.8
(2σ)				0.2	0.04	0.11	0.11	0.06	0.01	0.06	0.14	0.02	0	0
Exp MRB-29[d]				49.1	1.96	12.65	13.61	6.13	0.19	9.53	2.45	0.69	0.25	
Averages														
Mokulaevsky (Mk)n = 8[b]			0.55	48.7	1.20	16.43	12.80	6.83	0.19	11.42	2.00	0.30	0.10	1.82
Morongovsky (Mr2)n = 4			0.58	48.9	1.12	16.75	12.30	7.19	0.19	11.21	1.93	0.33	0.11	1.45
Morongovsky (Mr1)n = 6			0.56	49.4	1.10	16.29	12.40	6.90	0.18	11.29	1.95	0.38	0.11	1.87
Nadezhdinsky (Nd3)n = 2			0.57	50.4	1.01	16.50	11.45	6.57	0.18	10.99	1.93	0.84	0.15	1.65
Nadezhdinsky (Nd2)n = 10			0.56	52.2	1.06	15.95	11.18	6.07	0.16	10.08	2.15	0.98	0.12	1.67
Nadezhdinsky (Nd1)n = 11			0.59	52.2	0.94	16.38	10.24	6.32	0.16	10.33	2.35	1.00	0.10	2.76
TPBU n = 4			0.76	47.4	0.67	12.33	12.28	16.41	0.18	9.44	0.99	0.31	0.06	5.05
Tuklonsky (Tk)n = 9			0.66	49.6	0.88	15.70	10.97	8.99	0.17	11.11	2.10	0.34	0.08	3.77
GPBU n = 5			0.72	47.9	1.61	9.85	14.85	16.44	0.20	7.49	0.97	0.52	0.12	6.12
Gudchichinsky (Gd)n = 6			0.57	50.8	1.84	16.07	11.29	6.57	0.16	9.48	2.97	0.67	0.19	2.85
Syverminsky (Sv)n = 19			0.56	52.8	1.62	15.61	11.06	6.01	0.15	7.83	3.24	1.40	0.25	3.87
Ivakinsky (Iv)n = 9			0.37	51.7	2.26	15.41	13.73	3.55	0.19	6.95	3.47	1.98	0.75	2.52

geochemical variations are described in more detail elsewhere (Lightfoot et al. 1990b). Figure 2b shows similar data for section 1F. We note the following features:

(1) In core SG-9, there is a marked stratigraphic break between high mg-number, TiO_2, and Gd/Yb, and low La/Sm picritic basalts of the Gudchichinsky formation, and the low TiO_2, and Gd/Yb, and high La/Sm basalts of the Nadezhdinsky formation (Fig. 2a).

(2) In core SG-9, the Nadezhdinsky through Morongovsky formations exhibit a systematic change in, for example SiO_2, ε_{Sr}^{UR} and La/Sm with height, and at approximately constant mg-number (Fig. 2a and Lightfoot et al. 1990b). There is considerable scatter in Sr concentrations (Table 2 and Lightfoot et al. 1990b), but Ni and Cu together with the platinum group element abundances systematically increase upwards through this portion of the stratigraphy (Naldrett et al. 1992; Lightfoot et al. in prep.).

(3) In section 1F, there is a marked stratigraphic break between the Gudchichinksy picritic basalts and the low TiO_2 and Gd/Yb and negative ε_{Nd}^{CHUR} basalts of the Tuklonsky formation (Fig. 2b).

(4) In section 1F, the top formation is similar to the Nadezhdinsky formation in core SG-9. The chemostratigraphic variations which are characteristic of each formation and unit are summarised in Table 4 in terms of the features which best distinguish the formations and units.

Major and trace element variations

In Fig. 3a, the Lower Sequence basalts show a wide range in mg-number (0.32–0.74), and relatively high TiO_2 contents (1.3–2.4 wt%). In contrast, the Upper Sequence lavas have lower TiO_2 (0.45–0.95 wt%), and overlap in mg-number (0.51–0.76) with the Lower Sequence (TiO_2 = 1.0–2.5 wt%; mg-number = 0.3–0.76). The variations between the two sequences are not easily reconciled with different amounts of fractionation of a common magma, or melting of a common source (Lightfoot et al. 1990b). The Lower Sequence flows have high Zr/Y (5.5–9.0) and Ti/Y (250–670). Erlank et al. (1988) separate low and high-Ti magma types on the basis of Zr/Y ~ 6 and Ti/Y ~ 410. In this context, most of the samples in the Lower and Upper Sequences may be classified as high-Ti and low-Ti, respectively, in the context of the low- and high-Ti types within Gondwana CFB (Hawkesworth et al. 1984, 1986). The exceptions are the sub-alkalic Ivakinsky and tholeiitic Syverminsky lavas which have low Ti/Y (< 410) but relatively high TiO_2 contents (1.4–1.8 wt%, and 2.0–2.4

Table 2. (continued)

Depth (m)	Core/ Section (Sample no.	Ba	Rb	Sr	Y	Zr	Hf	Nb	Ta	Th	U	Co	Cu	Ni	Cr	Zn	Sc	V
128	1F(2)	941	48.5	380	45.0	365	9.13	28.8	1.47	n.a.	n.a.	27	18	12	32	149	20	122
197	1F(7)	712	60.0	480	26.8	203	5.29	16.7	0.96	n.a.	n.a.	33	39	52	210	94.0	22	165
249	1F(11)	806	44.7	424	25.0	201	5.00	15.1	0.85	3.41	0.94	34	30	58	210	91.0	21	170
308	1F(16)	303	13.3	170	23.5	187	4.30	13.4	0.67	2.20	0.57	35	28	41	178	95.0	23	189
329	1F(18)	31	1.3	138	14.9	89	2.46	6.2	0.36	0.58	0.17	89	134	883	970	100	20	205
377	1F(22)	125	6.3	265	16.3	61	1.78	2.8	0.17	0.63	0.16	47	110	101	386	72.0	32	236
454	1F(25)	135	0.8	266	14.5	58	1.71	2.6	0.57	0.57	0.14	44	86	87	310	67.0	30	213
484	1F(28)	233	4.9	256	14.9	67	1.79	2.9	0.18	0.78	0.18	48	97	103	383	66.0	29	223
512	1F(30)	124	8.7	127	11.3	50	1.37	2.2	0.12	0.52	0.12	73	61	298	900	69.0	7	177
525	1F(33)	100	4.7	140	8.1	29	0.78	1.1	0.07	0.32	0.08	71	44	259	850	60.0	7	153
565	1F(34)	278	28.2	238	19.6	119	3.06	7.2	0.45	2.42	0.57	39	42	35	235	74.0	30	203
666	1F(38)	1295	92.4	519	20.2	116	3.15	7.3	0.48	2.96	0.79	39	9	12	63	98.0	29	214
751	1F(41)	375	20.3	338	21.9	128	3.60	8.6	0.54	3.37	0.87	40	56	33	60	86.0	30	213
820	1F(44)	237	21.2	200	22.3	108	2.93	6.5	0.40	n.d.	n.d.	45	108	79	145	88.0	32	243
Obs MRB-29		314	13.91	303	24.92	174	4.72	13.9	0.83	2.32	0.54	47	151	99	265	107	30	293
2σ		16	0.36	6	0.31	5	0.33	0.3	0.04	0.13	0.04	1	10	3	7	12	2	5
Exp MRB-29		311	14.3	311	25.1	170	4.8	14.1	0.84	2.5	0.63	47	150	91	270	117	29	282
Averages																		
Mokulaevsky (Mk)		283	4	215	22.7	89	2.43	4.5	0.26	0.99	0.37	44	132	103	178	102	37	265
Morongovsky (Mr2)		304	6	207	22.3	89	2.43	5.1	0.32	1.07	0.45	42	122	107	171	97	35	249
Morongovsky (Mr1)		338	4	207	23.1	98	2.63	5.7	0.32	1.48	0.54	42	113	86	156	97	38	270
Nadezhdinsky (Nd3)		373	21	251	23.2	106	2.79	7.0	0.42	1.87	0.96	42	97	81	145	88	32	219
Nadezhdinsky (Nd2)		416	22	282	23.0	130	3.48	9.0	0.52	2.98	0.85	40	87	45	84	94	30	216
Nadezhdinsky (Nd1)		460	29	283	20.7	119	3.22	8.3	0.50	3.04	0.81	36	32	23	134	84	30	212
Tuklonsky TPBU		126	7	147	10.7	48	1.25	1.9	0.11	0.45	0.11	73	62	284	810	67	6	170
Tuklonsky (Tk)		199	4	249	15.3	63	1.76	2.7	0.18	0.64	0.16	47	101	110	393	68	30	224
Gudchichinsky GPBU		306	9	207	14.7	86	2.44	6.6	0.40	1.00	0.38	66	96	696	789	111	24	229
Gudchichinsky (Gd)		331	11	300	21.6	144	3.60	11.0	0.60	1.40	0.36	37	71	83	269	92	27	227
Syverminsky (Sv)		643	36	440	25.3	191	5.00	15.4	0.85	2.86	0.70	34	34	55	214	100	23	169
Ivakinsky (Iv)		900	36	458	43.5	315	7.78	27.2	1.37	5.43	1.30	26	23	18	41	152	22	140

wt%, respectively); we group these lavas with the high-Ti type based on their elevated TiO_2 contents. Furthermore, Gd/Yb and La/Sm exhibit marked changes between and within some of the formations (Fig. 3b), and indicate that the low-Ti basalts are unlikely to be interrelated simply by low pressure differentiation processes or small differences in the amount of source melting (cf. Lightfoot et al. 1990b).

Chondritic mantle normalised trace element abundance patterns for the average of each formation and unit (Fig. 4) indicate that the difference between low and high-Ti groups is accompanied by differences in the degree of heavy rare earth element (HREE) depletion, and the magnitude of P, Nb, and Ta anomalies. These fundamental differences are recorded in the shapes of the spider diagrams for the averages of both the picritic and tholeiitic members of the Gudchichinsky formation (A) and the picritic and tholeiitic members of the Tuklonsky formation (B). Ivakinsky and Syverminsky formations have features similar to the Gudchichinsky. The patterns of the formations above the Tuklonsky are in some cases broadly comparable in shape to the Tuklonsky (e.g. the Mokulaevsky). In detail, the Tuklonsky is less fractionated, has deeper Ta-Nb anomalies than the Mokulaevsky, and has lower ε_{Nd}^{CHUR}. In other cases (such as the Nadezhdinsky formation), groups of flows allocated to the lower (Nd_1), central (Nd_2) and upper (Nd_3) Nadezhdinsky have steeper patterns than the Tuklonsky and show differential degrees of light rare earth element (LREE) and large ion lithophile (LIL) element enrichment, which cannot be attributed to differentiation alone (Lightfoot et al. 1990b). However, these flows retain the negative Ti, Ta, Nb, and P anomaly of the Tuklonsky magma type, and presumably therefore retain a significant contribution from broadly similar source materials to the Tuklonsky magma type.

Isotope geochemistry

ε_{Nd}^{CHUR} and ε_{Sr}^{UR} values (Table 3), calculated at 248Ma (Renne and Basu 1991), range from + 7.4 to − 8.4 and from − 3.4 to + 66.8 respectively (Fig. 5a) which is similar to the range quoted by Sharma et al. (1991) and DePaolo and Wasserburg (1976) for basalts from the Noril'sk District and the larger Putoranian Province to the southwest. Basalts from the Nadezhdinsky through Morongovsky (Mr_1) display a broadly coherent upwards overall trend of decreasing ε_{Sr}^{UR} with increasing ε_{Nd}^{CHUR} (Fig. 2a), and then basalts from the Morongovsky (Mr_2) and Mokulaevsky have nearly constant Sr-, and Nd-isotope compositions. In detail, the lowermost Nd_1 samples are slightly less radiogenic than the central Nd_1 samples, and this links to a flattening of the La/Sm profile for Nd_1 lavas (Fig. 2a). The data are unusual in that the majority are displaced to high ε_{Sr}^{UR} relative to the mantle

Table 2. (continued)

Depth (m)	Core/ Section (Sample no.)	La	Ce	Pr	Nd	Sm	Eu	Gd	Tb	Dy	Ho	Er	Tm	Yb	Lu	La/Sm	Gd/Yb	Eu[e]
128	1F	49.13	113.5	12.75	55.21	11.68	2.40	10.6	1.58	9.14	1.78	4.67	0.66	4.25	0.61	4.21	2.49	− 16.8
197	1F	25.73	56.62	6.55	27.26	5.96	1.78	5.60	0.90	5.25	1.02	2.77	0.39	2.53	0.38	4.32	2.21	− 1.71
249	1F	22.48	51.43	6.00	24.90	5.65	1.77	5.22	0.80	4.87	0.99	2.35	0.36	2.30	0.35	3.98	2.27	− 0.39
308	1F	20.87	46.34	5.50	24.30	5.56	1.80	5.04	0.77	4.71	0.95	2.39	0.34	2.23	0.33	3.75	2.26	0.55
329	1F	5.94	16.24	2.31	11.51	3.25	1.09	3.37	0.51	3.07	0.59	1.38	0.20	1.18	0.17	1.83	2.86	0.05
377	1F	4.91	11.27	1.51	7.33	2.21	0.86	2.73	0.43	2.92	0.63	1.68	0.25	1.66	0.23	2.22	1.64	0.78
454	1F	5.90	13.19	1.63	7.99	2.15	0.86	2.59	0.42	2.83	0.57	1.65	0.25	1.52	0.23	2.74	1.70	1.18
484	1F	6.16	14.48	1.76	8.04	2.32	0.88	2.67	0.39	2.74	0.60	1.61	0.24	1.56	0.26	2.66	1.71	0.88
512	1F	4.54	10.34	1.34	6.28	1.85	0.71	2.02	0.32	2.13	0.46	1.29	0.18	1.17	0.18	2.45	1.73	1.00
525	1F	2.63	6.06	0.83	3.94	1.12	0.50	1.40	0.21	1.47	0.30	0.85	0.11	0.81	0.12	2.35	1.73	1.20
565	1F	16.19	35.91	4.12	16.32	3.80	1.05	3.74	0.56	3.65	0.78	2.02	0.29	1.98	0.30	4.26	1.89	− 2.50
666	1F	15.79	34.41	3.71	15.93	3.52	1.00	3.75	0.59	3.86	0.76	2.19	0.32	2.15	0.32	4.49	1.74	− 2.48
751	1F	18.30	39.31	4.72	18.52	4.10	1.10	4.20	0.62	3.90	0.87	2.23	0.32	2.20	0.32	4.46	1.91	− 3.42
820	1F	12.55	27.86	3.38	14.47	3.79	1.15	3.84	0.64	4.33	0.87	2.46	0.36	2.45	0.34	3.31	1.57	− 1.36
Obs MRB-29 (n = 4)-		20.52	49.55	6.09	26.48	6.18	1.88	5.72	0.82	5.21	0.99	2.52	0.37	2.34	0.35	–		
(2σ)		0.64	1.100.31		0.40	0.10	0.07	0.31	0.02	0.20	0.05	0.13	0.03	0.08	0.01	–		
Exp MRB-29 (n = 9)-		20.38	48.85	6.3	27.68	6.21	1.94	5.46	0.83	5.10	1.00	2.55	0.37	2.35	0.37	–		
Averages																		
Mokulaevsky (Mk)		7.04	16.80	2.04	11.13	3.20	1.12	3.74	0.64	4.06	0.88	2.52	0.37	2.32	0.36	–		
Morongovsky (Mr2)		7.33	17.13	2.06	10.62	3.02	1.05	3.63	0.64	4.08	0.88	2.54	0.35	2.32	0.35	–		
Morongovsky (Mr1)		9.07	20.75	2.39	12.39	3.27	1.07	3.80	0.65	4.08	0.87	2.53	0.36	2.33	0.36	–		
Nadezhdinsky (Nd3)		12.91	28.04	3.25	14.14	3.54	1.11	3.93	0.67	4.28	0.90	2.66	0.40	2.56	0.39	–		
Nadezhdinsky (Nd2)		17.33	37.65	4.17	18.18	4.13	1.16	4.16	0.68	4.22	0.90	2.48	0.36	2.34	0.35	–		
Nadezhdinsky (Nd1)		16.40	35.40	3.97	16.70	3.75	1.07	3.89	0.62	3.85	0.82	2.26	0.32	2.10	0.31	–		
Tuklonsky TPBU		4.03	9.27	1.20	5.55	1.59	0.64	1.91	0.29	2.02	0.42	1.18	0.17	1.10	0.17	–		
Tuklonsky (Tk)		5.53	12.68	1.60	7.59	2.15	0.85	2.63	0.42	2.85	0.60	1.63	0.24	1.57	0.24	–		
Gudchichinsky GPBU		6.42	16.66	2.29	11.57	3.21	1.12	3.46	0.54	3.09	0.60	1.54	0.20	1.24	0.17	–		
Gudchichinsky (Gd)		14.10	32.65	4.16	19.39	4.84	1.68	5.03	0.77	4.38	0.86	2.24	0.31	1.85	0.27	–		
Syverminsky (Sv)		22.81	50.79	5.83	25.72	5.74	1.80	5.34	0.83	4.96	0.99	2.58	0.37	2.42	0.35	–		
Ivakinsky (Iv)		44.99	100.61	11.10	51.38	10.88	2.99	9.86	1.51	8.59	1.70	4.49	0.62	3.92	0.57	–		

[a] mg-number = $(MgO/Aw_{MgO})/[(MgO/Aw_{MgO}) + (85*(Fe_2O_3)/100*Aw_{Fe_2O_3})]$

[b] n = number of analyses. Note: averages are based on a maximum of n analyses

[c] L.O.I. = loss on ignition. All major oxide concentrations are recalculated to 100% free of LOI and given in weight percent; trace element concentrations are given in ppm.

[d] not recalculated free of L.O.I.

[e] $Eu^* = CN_{Eu} - \frac{[CN_{Gd} + CN_{Sm}]}{2}$ where CN refers to the chondrite-normalised abundance of the REE.

Iv = Ivakinsky; Sv = Syverminsky; Gd = Gudchichinsky (GPBU = Gudchichinsky picritic basalt unit); Kh = Khakanchansky; Nd = Nadezhdinsky; Tk = Tuklonsky (TPBU = Tuklonsky picritic basalt unit).

n.d. = not determined or given

array defined by oceanic basalts (De Paolo and Wasserburg 1976). The magnitude of this shift cannot be explained by error in the assumed age because of the good stratigraphic control and reasonably well defined ages of stratigraphic units (Renne and Basu 1991). For example, an error in the age of 20Ma would only produce a shift of 3 epsilon units for Sr, assuming bulk earth $^{87}Sr/^{86}Sr = 0.7047$ and $^{87}Rb/^{86}Sr = 0.0816$. Considerable alteration of the Rb/Sr ratio and absolute abundance of large ion lithophile elements by hydrothermal fluids at the time of eruption, or closely thereafter may produce a shift in Sr isotopic composition, but cannot produce a shift of some 10 to 50 epsilon units to the right of the mantle array given the observed variations in Rb/Sr. The displacement to the right of the mantle-array is comparable to that observed in uncontaminated Deccan Trap lavas (Lightfoot et al. 1990a). The variation in ε_{Sr}^{UR} in the Nadezhdinsky-Kharayelakhsky sequence requires the preferential incorporation of radiogenic Sr, perhaps en-route through the crust (Lightfoot et al. 1990b), and/or contributions from material which had high Rb/Sr relative to Sm/Nd, and which was sufficiently old to have developed a range in isotope ratios (cf. Hawkesworth et al. 1983). Low-Ti CFB provinces tend to have relatively high Sr isotope ratios and low-Ti/Y, and in some areas this has been attributed to contributions from subducted sediments in the continental mantle lithosphere (Hergt et al. 1989a, 1989b, 1991).

The isotope ratios of the lower four formations (Iv, Sv, Gd, and Tk) are much more scattered (Figs. 2a, b). Ivakinsky and Syverminsky basalts also occupy small field displaced to the right of the mantle array, but at lower ε_{Nd}^{CHUR}. Both picritic and tholeiitic members of the Tuklonsky formation fall in a narrow compositional field which overlaps with the Ivakinsky data but are different from the

Table 3. Sr-, Nd-, and Pb-isotope data for Siberian Trap lavas from drill core SG-9 and section 1F, Noril'sk district, Russia

	Depth (m) (height in 1F)	$^{87}Sr/^{86}Sr$	ε_{Sr}^{UR} (248Ma)	$^{143}Nd/^{144}Nd$	ε_{Nd}^{CHUR} (248Ma)	$^{206}Pb/^{204}Pb$	$^{207}Pb/^{204}Pb$	$^{208}Pb/^{204}Pb$
						Present day values		
Core SG-9:								
	85.6 (Kh)	0.70466	3.9	0.51282	3.67	18.520	15.554	38.194
	294.5 (Mk)	0.70552	15.2	0.51264	0.64			
	414.0 (Mk)	0.70602	24.8	0.51265	1.39			
	557.0 (Mk)	0.70598	20.7	0.51267	1.68	18.701	15.564	38.300
	636.5 (Mk)	0.70574	18.2	0.51265	1.06			
	788.0 (Mr2)	0.70615	21.7	0.51271	2.30			
	819.0 (Mr2)	0.70541	15.6	0.51270	1.99	18.431	15.568	38.003
	1012.0 (Mr1)	0.70524	13.0	0.51272	2.38			
	1129.0 (Mr1)	0.70637	28.0	0.51263	1.15			
	1151.0 (Mr1)	0.70653	28.2	0.51257	0.14	18.416	15.554	38.173
	1271.0 (Nd3)	0.70714	31.5	0.51243	− 2.41			
	1300.0 (Nd2)	0.70756	42.8	0.51242	− 2.84			
	1337.0 (Nd2)	0.70900	57.6	0.51216	− 7.39	17.890	15.507	37.851
	1373.0 (Nd2)	0.70979	63.5	0.51214	− 7.81	18.247	15.549	38.261
	1491.0 (Nd1)	0.70966	66.8	0.51214	− 7.78			
	1546.0 (Nd1)	0.70953	65.1	0.51216	− 7.21			
	1591.0 (Nd1)	0.70968	60.0	0.51214	− 7.62	18.397	15.571	38.559
	1644.0 (Nd1)	0.70919	58.8	0.51212	− 8.20			
	1709.0 (Nd1)	0.70860	45.7	0.51218	− 6.91	18.681	15.570	38.532
	1761.0 (GPBU)	0.70686	32.8	0.51282	4.63	19.508	15.692	38.830
	1798.0 (Gd)	0.70692	30.9	0.51280	4.00	–	–	
	1821.0 (Gd)	0.70720	34.1					
	1841.0 (GPBU)	0.70765	31.5	0.51278	3.99			
	1862.0 (Gd)	0.70656	28.0	0.51243	− 2.29	18.298	15.564	38.279
	1887.0 (Gd)	0.70496	6.4					
	1931.0 (Sv)	0.70685	28.4	0.51247	− 1.34			
	1991.0 (Sv)	0.70719	31.1	0.51242	− 2.38			
	2045.0 (Iv)	0.70616	21.1	0.51242	− 2.10			
	2136.0 (Iv)	0.70651	17.4	0.51230	− 4.46			
	2200.0 (Yg)	0.70705	22.8	0.51255	0.66	19.117	15.821	38.312
Section 1F:								
Sample No.								
(2)	128 (Iv)	0.70737	26.0	0.51235	− 3.52	17.816	15.408	37.748
(7)	197 (Sv)	0.70690	19.8	0.51242	− 2.31	17.899	15.435	37.880
(11)	249 (Sv)	0.70676	20.7	0.51247	− 1.40	17.945	15.401	37.860
(16)	308 (Sv)	0.70645	20.3	0.51246	− 1.67	17.999	15.428	37.906
(18)	329 (GPBU)	0.70407	− 3.4	0.51297	7.36			
(22)	377 (Tk)	0.70584	19.7	0.51262	0.00			
(25)	454 (Tk)	0.70609	26.2	0.51235	− 4.59	17.577	15.365	37.444
(28)	484 (Tk)	0.70632	27.1	0.51241	− 3.75	17.439	15.384	37.395
(30)	512 (TPBU)	0.70662	24.1	0.51248	− 2.60	–	–	
(33)	525 (TPBU)	0.70652	27.8	0.51247	− 2.57	17.646	15.382	37.434
(34)	565 (Nd1)	0.70908	51.7	0.51216	− 7.64	17.965	15.429	38.077
(38)	666 (Nd1)	0.70886	63.8	0.51211	− 8.37	18.301	15.489	38.273
(41)	751 (Nd2)	0.70877	64.0	0.51213	− 7.99	18.064	15.445	37.976
(44)	820 (Nd3)	0.70754	31.7	0.51247	− 2.01	18.423	15.456	37.999
Other:								
SG–10	1515 (Yg)	0.70713	24.1	0.512510	− 0.03			
SG–18	1979 (TI)	0.70629	20.2	0.512650	1.24			
SG-18	1981 (TI)	0.70654	24.3	0.512410	− 3.37			
SG-2Ku	2554 (LTI)	0.70871	52.9	0.512270	− 5.64			
SG-2Ku	2572 (LTI)	0.70829	45.9					
SG-7Ku	2053 (Gd)	0.70475	4.6	0.512710	2.57			

overlying Nadezhdinsky through Mokulaevsky flows despite similar incompatible element ratios (Fig. 2b). Gudchichinsky basalts are quite different compared with the Tuklonsky; one Gudchichinsky picritic basalt from section 1F has $\varepsilon_{Nd}^{CHUR} = +7.31$ and $\varepsilon_{Sr}^{UR} = -3.4$, whereas two picritic basalts from core SG-9 have $\varepsilon_{Nd}^{CHUR} = +3.99$ and $+4.63$, $\varepsilon_{Sr}^{UR} = +31.5$ and $+32.8$, respectively. The tholeiitic members of the Gudchichinsky formation in core SG-9 have variable ε_{Nd}^{CHUR} (-2.3 and $+4.0$), but very different ε_{Sr}^{UR} ($+6.4$ and $+31.5$). Gudchichinsky lavas from 1F are characterised by elevated Ba, Rb, Sr and K_2O (but not Th or the light rare earth elements) compared with SG-9. Although it is possible that the variations in these analytes and Sr-isotopic signature were selectively changed in core SG-9 during alteration accompanying the emplacement of subsequent voluminous tholeiitic intrusions in the Noril'sk District such as the Talnakh Intrusion and the Low Talnakh Intrusion (Naldrett et al. 1992), it is unlikely that this affected only Gudchichinsky lavas.

Present day Pb-isotope ratios of the Siberian Traps (Fig. 5b) occupy a narrow range which is similar to the mid-Atlantic ridge basalts. Kharayelakhsky, Morongovsky, Mokulaevsky and Nadezhdinsky basalts have a remarkably uniform Pb-isotope signature ($^{206}Pb/^{204}Pb = 17.8$–18.8), yet have an enormous range in ε_{Sr}^{UR} ($+4.0$ to $+67.0$). Interestingly, Nadezhdinsky lavas have a slightly lower $^{206}Pb/^{204}Pb$ ratio compared with the Mokulaevsky despite their high La/Sm and SiO_2; this is very different from the contaminated Poladpur and Bushe Formations of the Deccan Trap which have elevated La/Sm, SiO_2, and a corresponding range of $^{206}Pb/^{204}Pb$ from 16.8 to 22.5 (Lightfoot and Hawkesworth 1988). Ivakinsky and Syverminsky lavas are displaced to slightly less radiogenic Pb-isotope ratios, and Tuklonsky tholeiites and picrites are some of the least radiogenic lavas yet characterised in the Siberian Trap sequence ($^{206}Pb/^{204}Pb = 17.4$–17.7). However, these are not as unradiogenic as, for example, the Mahabaleshwar lavas of the Deccan Trap, and the Parana high-Ti lavas, and it is interesting that the unradiogenic Pb of the Lower Sequence couples with higher Ti/Y. Gudchichinsky lavas show the widest range in Pb-isotope signatures, and picritic basalts from SG-9 are displaced to radiogenic Pb-isotope compositions. The Pb isotope data yield a broadly Archean model age 2.9 Ga on a broad scatter of data (Fig. 5b, 6).

Petrogenesis

The distinctive feature of many CFB is that they have radiogenic isotope ratios which are more extreme (lower $^{143}Nd/^{144}Nd$, higher $^{87}Sr/^{86}Sr$ and in some cases $^{207}Pb/^{204}Pb$) than those of oceanic basalts. Thus they contain at least a contribution from old, trace element enriched material which is widely accepted to be in the continental lithosphere (Hawkesworth et al. 1984). Some models invoke crustal contamination of magmas similar to those sampled in oceanic areas (Lightfoot 1985). Recently it has been argued that high-Ti CFB in the Karoo reflect mixing between depleted asthenosphere derived magmas and a lamproite-like component from the continental lithosphere (Ellam and Cox 1991). Low Ti CFB, such as those of the Siberian Traps, are unusual because in addition to their extreme isotope ratios, they are characterised by relatively low Ti, Nb, and Ta abundances which result in negative anomalies for these elements on chondrite normalised trace element diagrams (Fig. 4). Some of the high-Ti formations (e.g. Iv and Sv) also have negative Ta and Nb anomalies (Fig. 5a), and this could be attributed to crustal contamination (which is also consistent with the elevated SiO_2 and La/Sm of these rocks).

Figure 6 compares Ti/Y and Zr/Y ratios of the Siberian lavas with those of the Deccan (Cox and Hawkesworth 1985; Lightfoot and Hawkesworth 1988; Lightfoot

Footnotes to Table 3:
NBS987 gave $^{87}Sr/^{86}Sr = 0.71023$; the J&M Nd standard gave 0.511852 ± 15; BCR-1 gave 143Nd/144Nd = 0.51262. NBS981 and samples gave within run precisions of 0.035% (1σ)or better on $^{206}Pb/^{204}Pb$, 0.032% (1σ)or better on $^{207}Pb/^{204}Pb$, and 0.033% (1σ) or better on $^{208}Pb/^{204}Pb$. Beam currents for samples were 2.3-17pA. NBS981 gave $^{206}Pb/^{204}Pb = 16.901 \pm 0.021$ (1σ) $^{207}Pb/^{204}Pb = 15.444 \pm 0.0248$ (1σ), and $^{208}Pb/^{204}Pb = 36.554 \pm 0.0691$ (1σ) on ten determinations

$$\varepsilon_{Nd}^{CHUR} = \frac{[^{143}Nd/^{144}Nd_{Sample(t)}]}{[^{143}Nd/^{144}Nd_{CEUR(t)}]} - 1*10{,}000$$

$^{143}Nd/^{144}Nd_{CHUR(O)} = 0.51264$, $^{147}Sm/^{144}Nd = 0.1967$
$^{87}Sr/^{86}Sr_{UR(O)} = 0.7045$, $^{87}Rb/^{86}Sr = 0.0816$
$^{147}Sm = 6.54 \times 10^{-12}\ a^{-1}$, $^{87}Rb = 1.42 \times 10^{-11}\ a^{-1}$
(–) not determined. See Lightfoot et al. (1990b) for Rb, Sr, Sm and Nd concentration data for core SG-9 and Table 2 and Lightfoot et al. (in prep) for section 1F and other samples
Iv = Ivakinsky; Sv = Syverminsky; Gd = Gudchichinsky; GPBU = Gudchichinsky picritic basalt unit; Tk = Tuklonsky, TPBU = Tuklonsky picritic basalt unit; Nd = Nadezhdinsky; Mr = Morongovsky; Mk = Mokulaevsky; Kh = Kharayelakhsky
Yg = Yergalakhsky Intrusion; TI = Talnakh Intrusion; LTI = Low Talnakh Intrusion

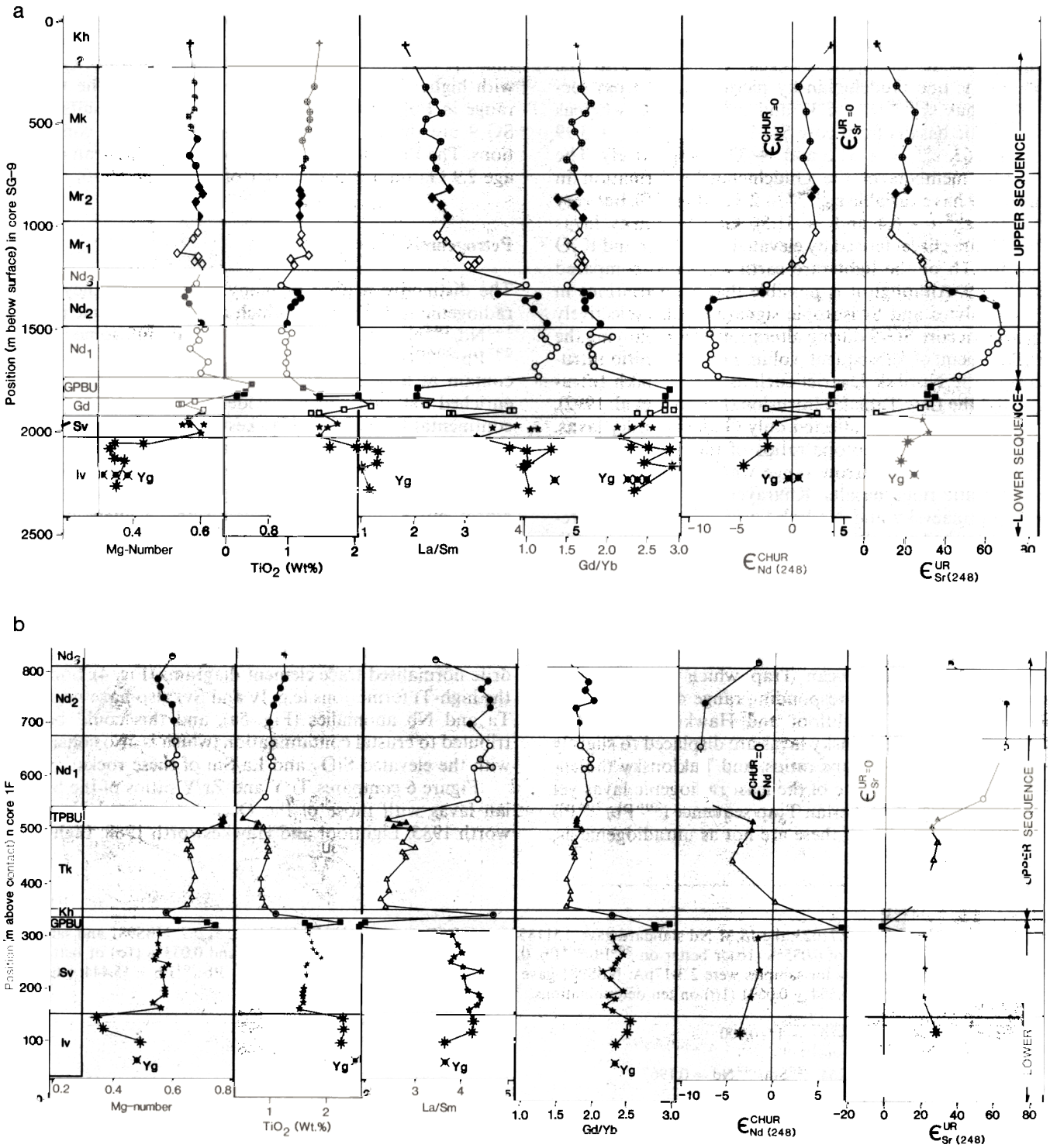

Fig. 2. **a** Geochemical stratigraphy of core SG-9 showing the variation in mg-number, TiO_2, La/Sm, Gd/Yb, Ta/La, ε_{Sr}^{UR}, and ε_{Nd}^{CHUR}. **b** Geochemical stratigraphy of section 1F showing the variation in mg-number, TiO_2, La/Sm, Gd/Yb, Ta/La, ε_{Sr}^{UR}, ε_{Nd}^{CHUR}. Mg-number $= MgO/Aw_{MgO}/(MgO/Aw_{MgO} + 85/100*Fe_2O_3/Aw_{Fe_2O_3})$. Iv = Ivakinsky, Sv = Syverminsky, Gd = Gudchichinsky, GPBU = Gudchichinsky picritic basalt unit, Tk = Tuklonsky (not developed in SG-9), TPBU = Tuklonsky picritic basalt unit, Nd = Nadezhdinsky (subdivided into three units – Nd_1, Nd_2, and Nd_3), Mr = Morongovsky (subdivided into two units – Mr_1 and Mr_2), Mk = Mokulaevsky and Kh = Kharayelakhsky

et al. 1990a), the Parana (Hawkesworth et al. 1986), and Tasmanian dolerites (Hergt et al. 1989a, b, 1991). The significance of this diagram is that it contrasts trends which are compatible with typical (oceanic) partial melting processes in the upper mantle (diagonal vector in Fig. 6), with those which require either a marked change in relative distribution coefficients, and/or contributions from other source materials (subhorizontal vector in

Table 4. Distinguishing geochemical features of the Siberian Trap lavas of the Noril'sk region, Russia

Formation/ Unit	mg-number[a]	Ni (ppm)	TiO_2 (wt. %)	La/Sm	Gd/Yb
Mokulaevsky (Mk)				< 2.4	< 1.8
Morongovsky (Mr)	< 0.6			2.2–3.2	< 1.8
Nadezhdinsky (Nd)				> 4.0	< 2.1
[b]TPBU	> 0.74			2.5–3.0	< 1.8
[c]Tuklonsky (Tk)	> 0.6			2.2–2.6	< 1.8
GPBU		> 490		< 2.7	> 2.3
Gudchichinsky (Gd)		< 120		< 2.7	> 2.3
Syverminsky (Sv)			< 2.0	> 3.1	> 2.1
Ivakinsky (Iv)			> 2.0	> 3.4	> 2.1

[a] $\text{mg-number} = \dfrac{\text{MgO}}{\text{Aw}_{\text{MgO}}} \Big/ \left[\dfrac{\text{MgO}}{\text{Aw}_{\text{MgO}}} + \dfrac{85^*(\text{Fe}_2\text{O}_3)}{100^*(\text{Aw}_{\text{Fe}_2\text{O}_3})}\right]$

[b] TPBU - Tuklonsky picritic basalt unit

[c] GPBU - Gudchichinsky picritic basalt unit

– criteria not required to distinguish basalt formations

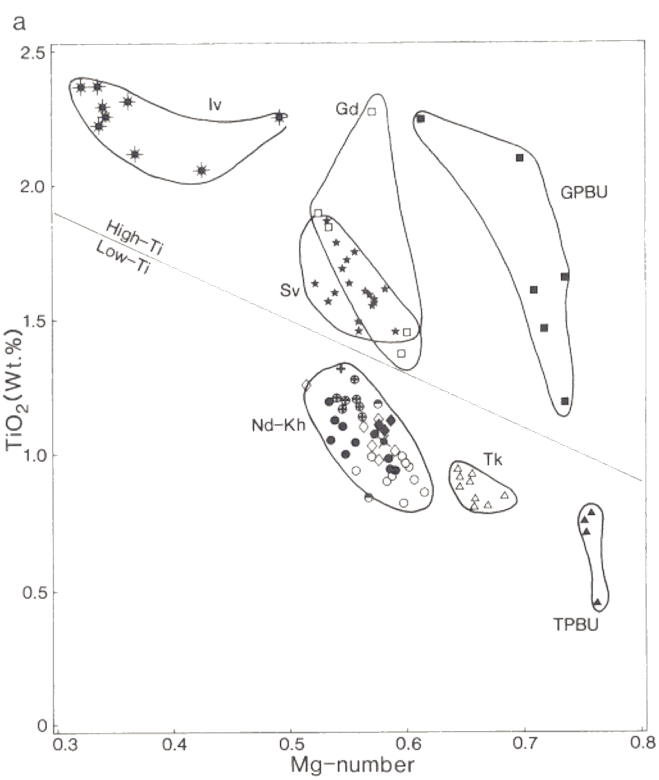

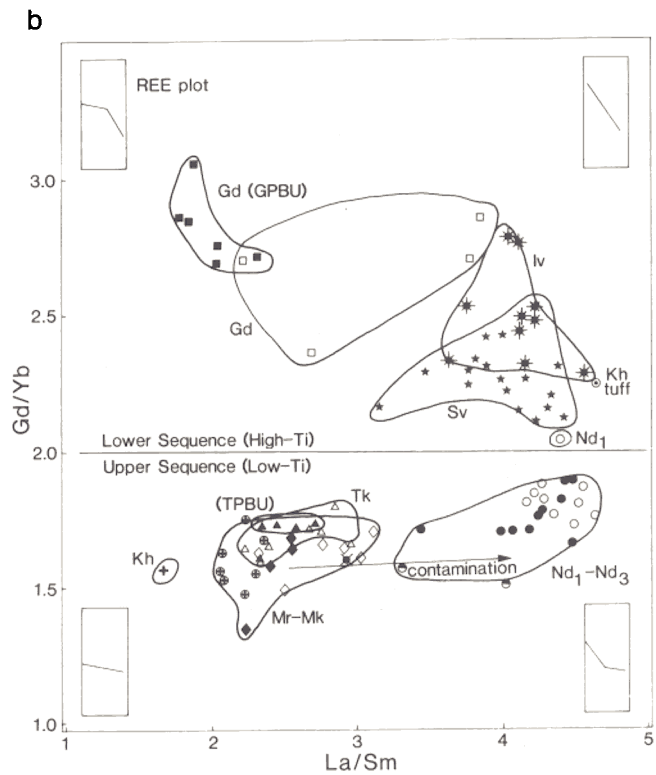

Fig. 3. a Variation in TiO_2 versus mg-number in all samples of Siberian Trap analysed by us (this study; Lightfoot et al. 1990b; Lightfoot et al. unpublished data). **b** Variations in La/Sm versus Gd/Yb in the same samples as Fig. 3a

Fig. 6). During partial melting in the upper mantle the bulk partition coefficients for Zr, Ti, and Y are in the order $D_{Zr} < D_{Ti} < D_Y$, and this is especially marked if garnet is a residual phase (Pearce and Norry 1979). Variations in the degree of partial melting thus tend to generate positive arrays on Fig. 6, and the fields of the Gudchichinsky, Tuklonsky and Mokulaevsky lavas of the Siberian Trap, fields for the Deccan Trap and the high Ti/Y Parana basalts are consistent with variable degrees of partial melting of source regions with similar Ti/Y and Zr/Y with the Gudchichinsky lavas being the smallest degree melts. The degree of melting must be sufficient to generate picritic liquids, yet leave garnet as a residual phase in order to fractionate Ti/Y (i.e. about 10% melting). Moreover, since lamproites are small percent melts with high incompatible element contents, the high Ti/Y Parana fields could, at least on the basis of this diagram, also be generated by mixing between a depleted mantle melt and a lamproitic end-member. The Gudchichinsky lavas fall on a trend of increasing Ti/Y with Zr/Y (called the mantle trend), and even though their Sr-isotope signatures are anomalous, they are unlikely to contain a lamproitic

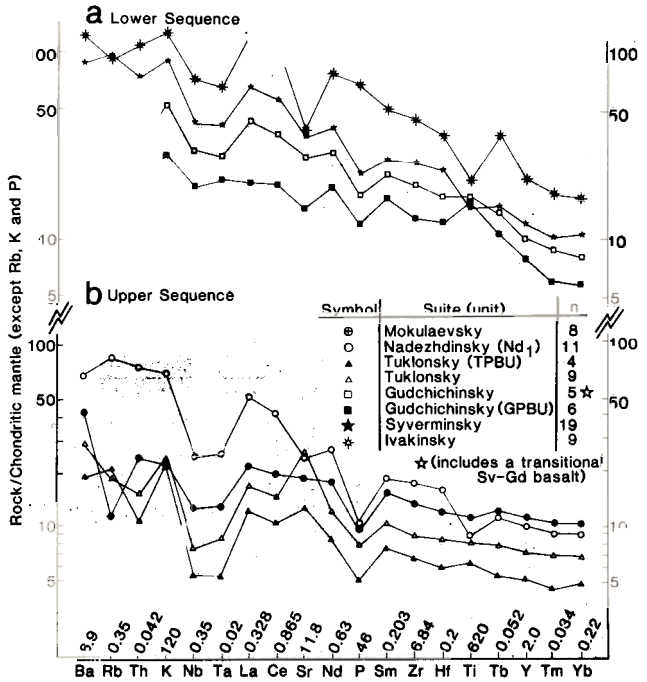

Fig. 4. Chondrite-normalised variations in formations from the Lower Sequence (*a*) and the Upper Sequence (*b*). Averages are based on all of the data available (this study; Lightfoot et al. 1990b; Lightfoot et al. unpublished data). The marked negative Ti, Ta, and Nb anomalies in the Mokulaevsky and Nadezhdinsky are features of the continental lithosphere

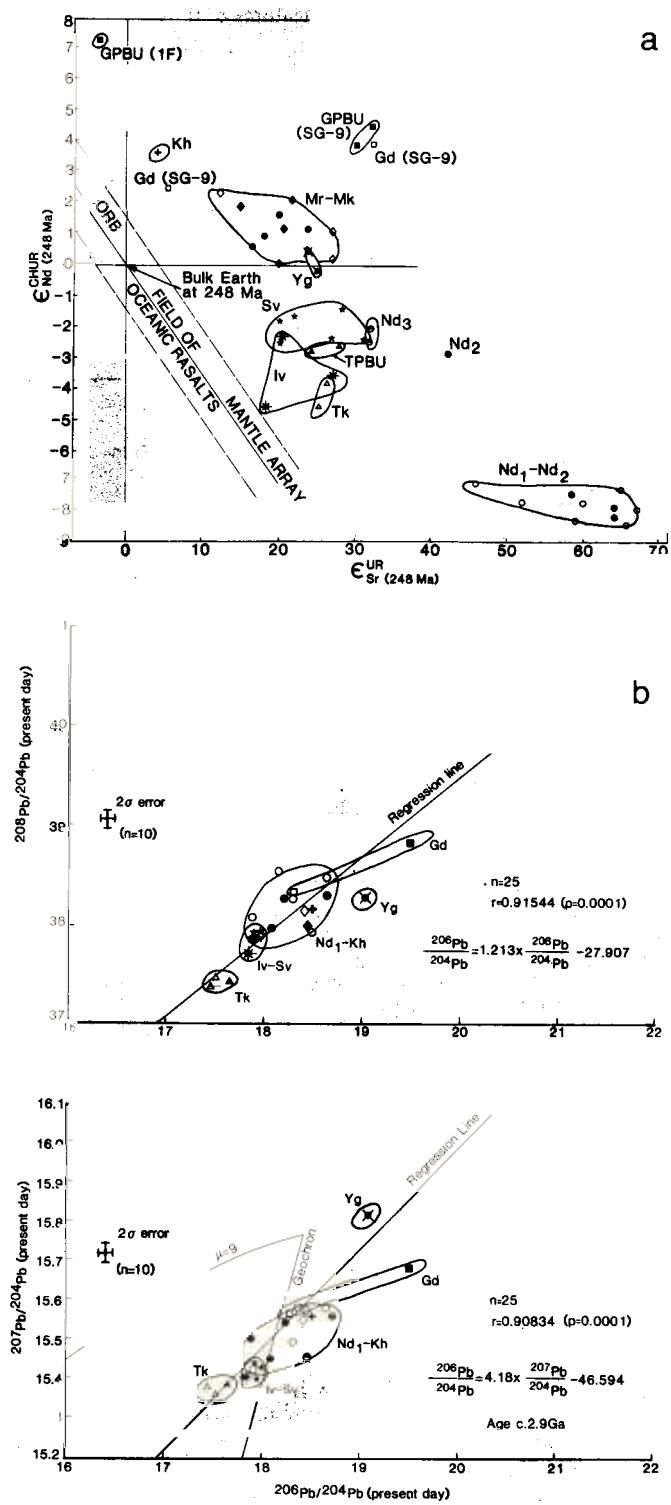

Fig. 5. **a** ε_{Nd}^{CHUR}-ε_{Sr}^{UR} variations in Siberian Trap lavas showing the tight trend of the Upper sequence, and the displacement of this array to the right of the mantle array. **b** Variations in $^{208}Pb/^{204}Pb$ versus $^{206}Pb/^{204}Pb$ and $^{207}Pb/^{204}Pb$ versus $^{206}Pb/^{204}Pb$ in Siberian Trap lavas

contribution. The low-Ti, low-K Nuanetsi picrites from the Karoo Volcanic Province plot very close to the field of the GPBU on Fig. 6 (data from Ellam and Cox 1991).

Mokulaevsky and Tuklonsky lavas fall close to or within the field of rocks derived from the asthenospheric mantle similar to the source of ocean island basalts, and Tuklonsky lavas have higher Ti/Y and Zr/Y than Mokulaevsky lavas. The different Nd and Sr isotope ratios of Tuklonsky and Mokulaevsky magmas preclude a partial melting relationship between these lavas, and suggest that two or more source components contributed during the melting process.

In sharp contrast to the fields for such relatively high Ti CFB, the rocks from the low Ti CFB (Nadezhdinsky and Morongovsky formations of the Siberian Trap), low-Ti Parana basalt and the Tasmanian dolerites are displaced to high Zr/Y at low Ti/Y (Fig. 6). These data are not readily explained by models of variable partial melting, or of mixing with a very small percentage of lamproitic upper mantle melts. Rather the combination of low Ti/Y, and hence negative Ti anomalies on mantle normalised trace element diagrams (Fig. 4b), are a feature of granites and sediments from the upper continental crust (Taylor and McLennan 1985). These relatively low Ti abundances are also associated with negative Ta and Nb anomalies (Fig. 4b), and relatively high Sr isotope ratios (Fig. 5a), and they would therefore appear to be indicative of a significant contribution from upper crustal material in the generation of low Ti CFB. At issue is whether that crustal material was introduced by contamination processes en route through the crust, whether it had been previously introduced to source regions in the mantle lithosphere by subduction, or by both processes. Unlike the more incompatible elements, the abundances of Zr, Ti,

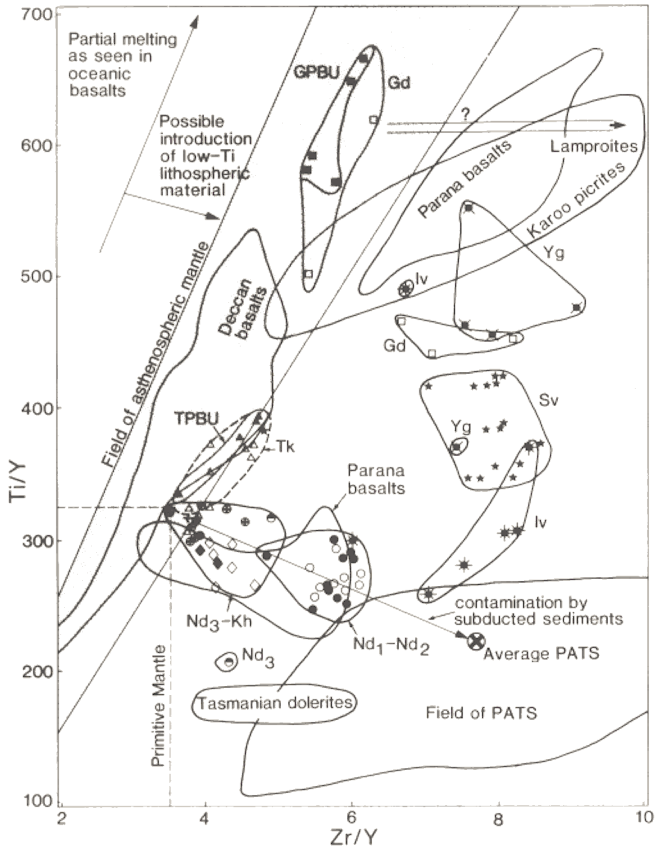

Fig. 6. Ti/Y-Zr/Y variations in Siberian Trap lavas showing the Lower Sequence formations on the trend defined by melts of four phase garnet lherzolite, and the upper formations displaced to high Zr/Y and low Ti/Y which is a feature of the continental lithosphere. See text for data sources. Field of post-Archean shale is based on Taylor and McLennan (1985)

and Y are similar in many mantle derived magmas and crustal rocks. Thus to generate negative Ti anomalies by the addition of crustal material to basaltic magmas requires high degrees of crustal contamination (e.g 25% contamination with crustal material containing 0.5% TiO_2 of a basalt with 1.2% TiO_2 only reduces its TiO_2 content by 0.175%). It follows that while many authors have been prepared to invoke crustal contamination processes to explain the more extreme LILE contents (Lightfoot et al. 1990b) and isotope ratios of the low Ti CFB, it has rarely been argued that their negative Ti (and Ta, and Nb) anomalies are due to such effects unless the amount of contamination was extremely large. Hergt et al. (1991) overcame the problems raised by such mass balance considerations by proposing that the upper crustal signature in the low Ti CFB of the Tasmanian dolerites was due to the introduction of subducted sediments to their upper mantle source regions during an ancient episode of subduction. Their calculations demonstrated that ~3% sediment in the source regions of such basalts produced similar isotope and trace element signatures to 25–35% crustal contamination of low-Mg basaltic magmas.

Negative Ta and Nb anomalies are much more common in continental than in oceanic within plate rocks and thus they have often been taken as an indication of contributions from the continental lithosphere. The development of such anomalies can be illustrated by variations in Nb/La, and Fig. 7a-c summarises variations in Ti/Zr, Nb/La, ε_{Nd}^{CHUR}, and La/Sm for the Siberian Traps. Mokulaevsky through Nadezhdinsky lavas fall on a trend of falling Ti/Zr as La/Sm increases (Fig. 7a). Gudchichinsky lavas have the highest Nb/La of the basalts analysed, and Ivakinsky and Syverminsky lavas fall on a trend of declining Ti/Zr and Nb/La as La/Sm increases. Tuklonsky formation lavas fall in the field of asthenospheric mantle-generated lavas on Fig. 6, but have remarkably low Nb/La (< 0.57) and La/Sm (< 3) which appears to preclude a simple asthenospheric mantle source for these lavas. This also indicates that lavas displaced to low Nb/La need not have markedly high Zr/Y and low Ti/Y ratios typical of contaminated lavas (Fig. 6). In the Tuklonsky there is a range in Nb/La from values similar to those of primitive mantle and many oceanic basalts, to low values indicative of marked negative Ta and Nb anomalies (Fig. 4B). Since such negative anomalies are not a feature of oceanic basalts, they are also inferred to reflect contributions from the continental lithosphere. The low Nb/La rocks *also exhibit a range in La/Sm* (Fig. 7a), and La/Sm in turn varies systematically with Nd isotopes (Fig. 7c), so that it may be further concluded that the lithospheric contributions in these basalts were characterised by variable REE and $^{143}Nd/^{144}Nd$ ratios. Finally, the correlation between Ti/Zr and La/Sm (Fig. 7b) is even more striking than that between Nb/La and La/Sm (Fig. 7a), suggesting that although the development of negative Ti and Ta and Nb anomalies both reflect lithospheric contributions, some process has fractionated Ti/Nb. Nedezhdinsky, Morongovsky and Mokulaevsky lavas fall on a broad array of decreasing Nb/La with increasing La/Sm and falling ε_{Nd}^{CHUR} as $^{147}Sm/^{144}Nd$ declines (not shown). The Tuklonsky lavas are displaced below this array, whereas Gudchichinsky lavas are displaced above this array. The slope of the ε_{Nd}^{CHUR} versus $^{147}Sm/^{144}Nd$ array yields a very approximate model age of 2.4 Ga.

Low Nb/La basalts have variable La/Sm and $^{143}Nd/^{144}Nd$ (Fig. 7b and c). It is important to emphasize that the variations between Nb/La and other trace element and radiogenic isotopes are decoupled, and must therefore reflect at least two different processes. The available evidence suggests that one of these processes involves the addition of crustal material to continental lithospheric mantle, and we would argue that this process could be responsible for the development of suitable sources for low Nb/La lavas with radiogenic Sr-isotopic compositions (i.e. Nd_1–Nd_2). As a broad illustration of this point, Fig. 7b shows that the general decline in the Nb/La ratios of the Nd_1 source can be generated by 15% addition of post Archean terrestrial shale (PATS – Taylor and McLennan 1985) to a source which has a comparable La/Sm and Nb/La to the asthenospheric upper mantle (e.g. taken to be N-MORB source, from Sun and McDonough 1989, for the purpose of this calculation). The calculations are model-dependent, and lowering the abundances of Ta, La, and Sm in the source in a constant ratio can reduce the amount of sediment required to generate Nd_1 sources to 5%. The depth of the Nb anomaly (Fig. 4) in Nd_1 lavas approach that of PATS, and therefore 15%

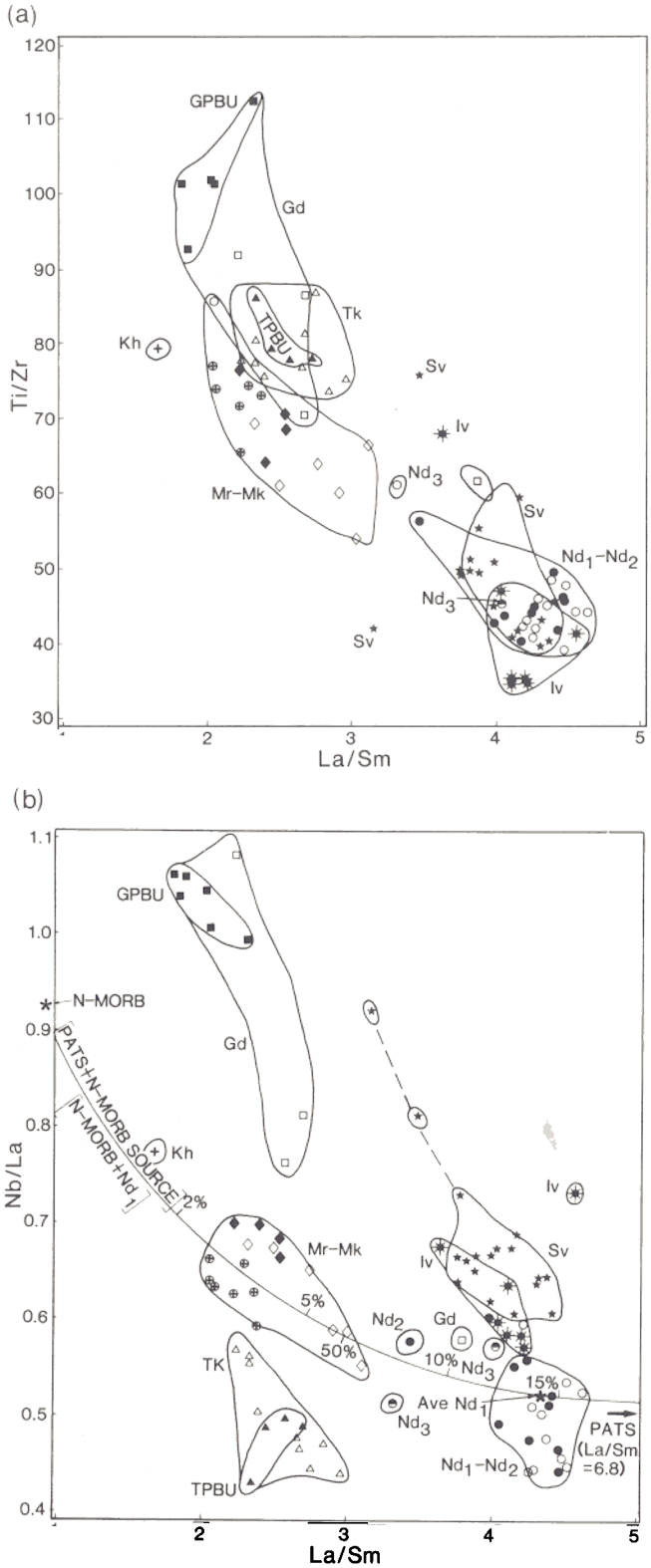

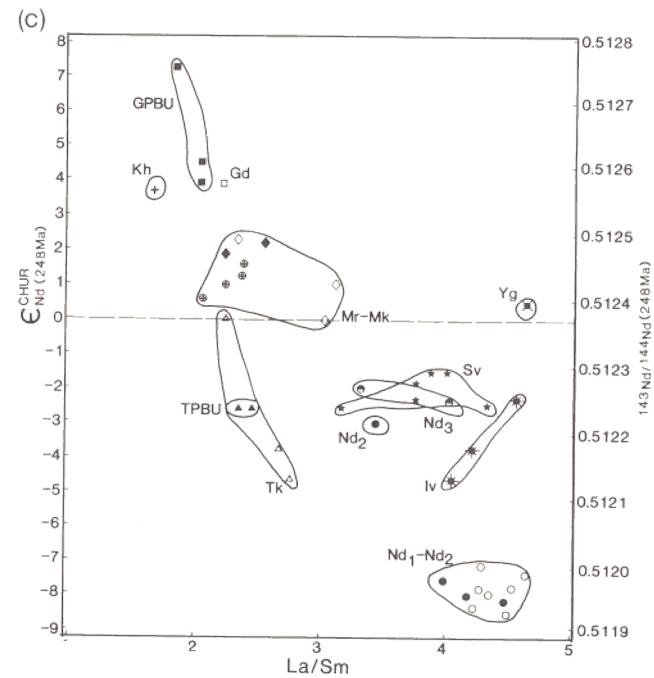

Fig. 7. **a** Ti/Zr versus La/Sm in Siberian Trap lavas. **b** Nb/La-La/Sm variations in Siberian Trap lavas. Partial melting processes should generate a positive array on this plot; the rocks actually plot in a broad field with negative slope. N-MORB source is calculated based on a source which has 4x lower Nb, La, and Sm compared with N-MORB of Sun and McDonough (1989). PATS is from Taylor and McLennan (1985), p. 28 (ave. 1). **c** ε_{Nd}^{CHUR}-La/Sm variations in Siberian Trap lavas

PATS is very much an upper limit unless the end-member compositions are unrepresentative.

An extension of this argument is that Mokulaevsky and Morongovsky lavas can be produced by contamination of a source or magma comparable in composition to N-MORB source by PATS, and the amount of contamination based on this model is ~5%. In detail, the array of Nd-Mr lavas points to a different asthenospheric component from the GPBU which has higher Nb/La than E-or N-MORB (i.e. more like oceanic island basalts). It is hard to argue that Nd_{1-2} lavas are derived entirely from a lithospheric mantle source, as a particularly unusual process would be required to generate wholesale melts from the continental lithospheric mantle. Presumably these lavas contain a more recent asthenospheric component, with the lithospheric component falling on the array to the right of the field of Nd_{1-2} in Fig. 7c. Mixing between magmas with extreme Nd_1 signatures (i.e. lithospheric mantle) and asthenospheric melts with low Nb/La (i.e. MORB-type) compositions can explain the intermediate compositions of Mr and Mk lavas by mixing of, for example, up to 40%-N-MORB with 60% Nd_1 lava.

What this model cannot explain is the very low Nb/La and La/Sm of the Tuklonsky lavas as PATS has a high La/Sm of 6.8, and addition of PATS to N-MORB source cannot generate such an extreme hyperbolic mixing array. In the case of the Tuklonsky rocks, a different source component is required which has both low Nb/La and La/Sm, but is also characterised by relatively high Ti/Zr and this was not the same source material as that contributing to the Nd_1-Mk series lavas.

Discussion

Recent debates on the generation of CFB have focused on the causes of such large volume magmatic events, on the

nature of the asthenospheric and lithospheric end-members, and on their relative contributions. Thermal considerations effectively require the presence of anomalously hot mantle, as in mantle plumes (White and McKenzie 1989), and that in turn should result in relatively high degrees of partial melting. High Mg basalts are present in Nuanetsi in the Karoo (Ellam and Cox 1991) and Deccan (Krishnamurthy and Cox 1977), but in general they are rare in CFB formations because most lavas which reach the surface have undergone significant fractionation at shallow levels. The Nuanetsi high Mg rocks are different from most of the Siberian Trap of the Noril'sk District (excluding the GPBU) because, in addition to slight negative Ta and Nb anomalies and ε_{Nd}^{CHUR} values, they have high Ti/Y, Zr/Y and incompatible element contents. Thus they contain a significant contribution from lithospheric sources, and this has been modelled by the introduction of small degree lamproitic melts from the continental mantle lithosphere (Ellam and Cox 1991). What is unusual about the Siberian Traps is that they include high Mg basalts, and those basalts include ones which have not only been *least* influenced by a contribution from lithospheric material (i.e. the Gudchichinsky lavas) but also ones which have been more strongly influenced by a contribution from the lithosphere (i.e. the Tuklonsky-Nadezhdinsky lavas).

In detail two groups of picrites have been identified which have tholeiitic analogues. The Tuklonsky formation picrites and tholeiites exhibit a lithospheric signature which is a feature of most of the Siberian basalts from the Noril'sk district, whereas the Gudchichinsky picrites and tholeiites have Nd-isotope and trace element ratios more consistent with derivation from the sub-lithospheric mantle. As illustrated in Fig. 7a the sampled GPBU plots slightly above the main array for the Nadezhdinsky-Mokulaevsky basalts but arguably on a curved trajectory. This curved array could be interpreted in terms of mixing between a lithospheric end-member with low Ti/Zr (< 40), and an asthenospheric end-member with Ti/Zr ~ 90 and Ti/Y ~ 305, and the difference in Ti/Y and Zr/Y between the asthenospheric end-member and the Gudchichinsky rocks would then be taken to reflect differences in the degree of partial melting, with Gudchichinsky rocks representing smaller percent melts ($\leq 10\%$ melts of MORB type source). The nature of the asthenospheric end-member for the main upper sequence array (Nd-Mr-Mk) can be further inferred from the variations in Nd isotopes and trace element ratios. Assuming that such an end-member has an ε_{Nd}^{CHUR} value of $+7.36$ (represented by the most radiogenic GPBU basalt), the variation of ε_{Nd}^{CHUR} with La/Sm (Fig. 7c) indicates that the La/Sm ratio is ~ 1.5 in the high ε_{Nd}^{CHUR} component. Such values are more depleted than those of chondritic mantle (1.65), and so it is inferred that the asthenospheric material involved in the upper sequence basalts (Tk-Nd-Mr-Mk) had somewhat more MORB-like rare earth element (REE) and high field strength element (HFSE) ratios.

Due to the high TiO_2 content of the Gudchichinsky compared with the Upper Sequence lavas, and the difficulty of using this end-member in explaining the lower inferred Ti/Zr and Nb/La ratios of the asthenospheric end-member (Fig. 7a-b), we must attempt to reconstruct the geochemical fingerprint of the asthenospheric end-member of the Nd-Mr array. We do this by making the implicit assumption that the asthenospheric end-member has high ε_{Nd}^{CHUR} and no Ta-Nb anomaly. Extrapolating the trend of the Nd-Mr data array on a plot of ε_{Nd}^{CHUR} versus Ta/Sm, we find that Ta/Sm is chondritic (0.1) at $\varepsilon_{Nd}^{CHUR} = +7$ which is a reasonable value for oceanic basalts. Assuming that these values typify the source, we can evaluate normalised abundances of the other incompatible elements by plotting element/Sm versus Ta/Sm and reading the values on the Nd-Mr array at Ta/Sm = 0.1.

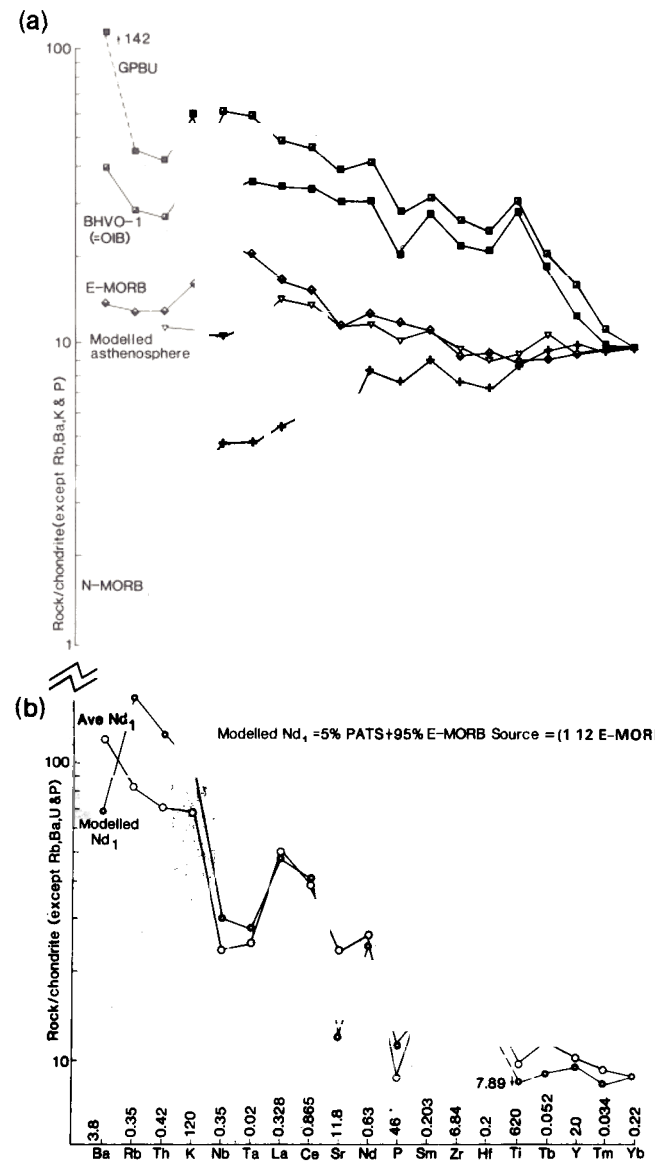

Fig. 8. Chondrite-normalised (Thompson et al. 1983) variations in: **a** modelled asthenospheric source of Nd_1-Mr_1 lavas compared to the composition of GPBU (this study), OIB as represented by BHVO-1 (Sun et al. 1979), N-MORB and E-MORB (Sun and McDonough 1989), and **b** the Nadezhdinsky (Nd_1) modelled by the combination of E-type MORB source (= 1/12 E-MORB) (Sun and McDonough 1989) and PATS (Taylor and McLennan 1985) in a 5:95 ratio where abundances in modelled Nd_1 have been normalised to Yb of actual Nd_1

We recalculate chondritic abundances and plot them in Fig. 8A where data are double normalised to $Yb_N = 10$. We do not show values for Ba, Rb, and K because the scatter of the array reduced the sensitivity of the plot to the ratio of the end-member. For comparison, we show the compositions of ocean island basalt represented by BHVO-1 (Sun et al. 1979), N-MORB and E-MORB (Sun and McDonough 1989). This plot demonstrates that the modelled asthenospheric component is LILE and LREE depleted relative to OIB and the GPBU (which have comparable patterns, except for Ba and K), but are LILE and LREE enriched with respect to N-MORB. The closest comparison on the basis of ratios is between the modelled asthenospheric component and E-type MORB, but the LILE and LREE are slightly depleted compared to this source.

In detail, the Tuklonsky and debateably the Mokulaevsky lavas fall on a different array to the Nd-Mr lavas (Fig. 7b), which in turn suggest that the asthenospheric component has mixed with components from the lithosphere with similar Nb/La but different (or a range of) La/Sm and ε_{Nd}^{CHUR}.

Several simple models have been explored to explain the range in isotope and trace element compositions in the upper sequence rocks. The most straightforward involves direct contamination of mantle-derived magmas by the continental crust within the feeder-conduit system (Lightfoot et al. 1990b). However, this model still requires that the least contaminated Mokulaevsky-type magma has itself a significant contribution from the continental crust. Modelling of the most contaminated Nd_1 lavas based on an Mokulaevsky-parent magma type requires the addition of up to 40% tonalite (Lightfoot et al. 1990b). Assuming a low LILE picritic precursor to the Mokulaevsky, the amount of tonalite is reduced. Recent modelling has shown that the composition of Nd_1 lavas can be produced by adding as little as 8% granodiorite (average Bolgokhtoksky intrusion-Fig. 1) to Tk tholeiite with subsequent olivine, augite, and plagioclase fractionation. This model will be explored elsewhere (Lightfoot et al., in prep.) but we note that there is still a requirement to generate the particularly unusual geochemistry of the parental Tuklonsky lavas, and these may have directly to sample a different source from the Mokulaevsky lavas.

Interestingly, intrusive portions of the trap which carry comparable incompatible element and isotope ratios to Nd_1 lavas (namely the Low Talnakh Sill-Naldrett et al. 1992 and Table 3) are more mafic and have not fractionated as far as Nd_1 lavas. This has an important bearing on the timing of contamination relative to magma evolution, and data for this intrusion (which has not differentiated significantly in-situ) suggest that contamination occurred before this magma became as evolved as the Mokulaevsky lava (e.g. Mk: Nb = 4.5ppm and Low Talnakh Sill:Nb = 2.5ppm). Thus, assuming that contamination of a more mafic magma occurred, the percentage of crust is reduced considerably. Models using a tonalite with 19ppm Nb and a lava with 4.5ppm Nb (= Mk) require 26% crust, whereas this is reduced to 10% crust for a magma with 2.5ppm Nb, which compares with the average Low Talnakh Intrusion magma composition of Naldrett et al. (1992).

Using an uncontaminated low-Mg basalt derived from the asthenospheric mantle rather than Mk magma, the amount of PATS required is larger. Although mechanisms can be found to change incompatible and isotope ratios through complex open system processes (such as RTF magma chambers), virtually no fractionation appears to accompany this process as the mg-number remains almost constant in the Nadezhdinsky-Mokulaevsky sequence. It is therefore appropriate to investigate the extent to which these variations were inherited from the source(s).

Mixing between large volume asthenosphere derived magmas and small percentage melts from the mantle lithosphere has been proposed for the Karoo volcanics of the Nuanetsi area (e.g. Ellam and Cox 1991). However, such melts tend to have high Zr/Y and Ti/Y ratios and so they are not suitable end-members for low-Ti basalts such as the Nd-Mr-Mk array on Figure 4A. Simple mixing between N-MORB magma (Sun and McDonough 1989) and average post-Archaean terrestrial shale (PATS) (Taylor and McLennan 1985) requires 60% bulk PATS and 40% N-MORB to produce the Zr/Y ratios of the Nd_1 basalts. A mixing model adequately accounts for the shape of the REE and HFSE patterns of the Nd_1 rocks (Fig. 4B), but it requires unrealistically large amounts of bulk sediment to be introduced to the MORB type magma. Assuming a mantle end-member which is more primitive, this value drops, but the amount of PATS required for a 10% melt of N-MORB source is still $\sim$20%. A third group of models seeks to introduce what appears to be the distinctive REE and HFSE signature of a sedimentary component into the source regions of the basalts prior to melting. This greatly reduces the amount of sediment required, but the observed LIL/HFSE ratios can only be achieved if the mantle component has lower incompatible element contents than MORB-type mantle. A good fit of the Nd_1 data is achieved by mixing between PATS and residual mantle with a primitive E-type MORB source signature, and in this model the amount of sediment is $\leq$ 5% (Fig. 8). Similarly, 1–2% addition of PATS to E-MORB source can generate lavas with Mokulaevsky trace element signatures.

Recent debates on the role of mantle plumes beneath lithospheric mantle in the generation of CFB (White and McKenzie 1989; Campbell and Griffiths 1990; Hill 1991) have identified the probable importance of asthenospheric magmas in the makeup of many flood basalt magmas. The question remains whether lithosphere can in itself be a significant source (Ellam and Cox 1991; Hill 1991). Geophysical data (Campbell and Griffiths 1990) argue against a lithospheric source on the basis of its low temperature and the extremely high temperature required in asthenospheric melts. Ellam and Cox (1991) argue that an average contribution of 20% from the mantle lithosphere is required to explain the Nuanetsi rocks, but we see no geochemical evidence for a lamproitic component in the studied sequences of Siberian Trap lavas although lamproites are known in the Siberian Trap.

Recent models of dehydration melting in the formation of CFB indicate that, particularly in the presence of elevated temperatures above mantle plumes, melting of lithospheric mantle in the presence of small amounts of water may produce significant volumes of magma

(Gallagher and Hawkesworth 1992). Gallagher and Hawkesworth's model predicts that lithospheric melts will dominate in the early stage of flood basalts events. Figs. 2a and b suggest that an asthenospheric signature is predominant in the lower lavas. However, as this activity is concentrated on the Noril'sk-Kharayelakh and North Kharayelakhsky faults, which appear to be very deep structural features, the magmas reaching the surface in this region may not be typical of the flood basalts as a whole. The fact that the most radiogenic Sr in Nadezhdinsky lavas is accompanied by a wide range in SiO_2 (49–55 wt%) may indicate that wet melting may be important in the generation of lavas from within the lithospheric mantle.

Summary and conclusions

In summary, the flood basalts of the Siberian Traps at Noril'sk exhibit many of the isotope and trace element characteristics of the Mesozoic high- and low-Ti flood basalts associated with the break-up of Gondwanaland. They are unusual in that through most of the succession (Nd-Mr-Mk) there is a progressive decrease in the signature of material from the continental lithosphere. They include two types of high-Mg picritic lavas (GPBU and TPBU) together with tholeiitic analogues with trace element ratios similar to oceanic basalt asthensopheric sources (i.e. Gd and Lower Sequence flows) and melts containing a significant contribution from the continental lithosphere (Tk and Upper Sequence flows). Significantly, however, the erupted Gudchichinsky picrites do not plot on the geochemical arrays from the main, upper sequence rocks (e.g. Fig. 4A), and the Tuklonsky picrites are slightly displaced to higher Ti/Y. Thus it is argued that the Gudchichinsky picrites represent smaller percentage ($< 10\%$) melts than any asthenospheric end-member involved in the generation of most of the Siberian basalts in the Noril'sk district, and that the latter had much more depleted trace element ratios and abundances. Tuklonsky picrites have comparable Ti/Y and Zr/Y to asthenospheric melts, but very low Nb/La and negative ε_{Nd}^{CHUR} which makes them different from the Gudchichinsky, and more like the overlying Nd-Mk flows which contain a significant contribution from the mantle lithosphere. The lithospheric component is not readily reconciled with the introduction of a small percentage of lamproitic melt, but rather it has the distinctive trace element signature of upper crustal rocks. Mass balance considerations may preclude suggestions that all of this material was simply introduced to magmas en route through the crust unless the degree of contamination was large and involved extremely primitive lavas, but they are consistent with a small contribution from subducted sediment in the source of such low-Ti CFB (Hergt et al. 1991). An asthenospheric component comparable with an enriched MORB source is recognised as an end-member to the Upper Sequence and this component is geochemically different from the high-Ti asthenospheric component in the Lower Sequence which resembles OIB magma. Neither the Lower nor Upper Sequences has trace element or isotopic signatures characteristic of the main mass of Purorana lavas, and it is suggested that the Noril'sk lavas are quite distinctive from the main Siberian Trap sequence.

The plume model for CFB accounts for the eruption of the varied sub-alkaline to picritic Lower Sequence flows at Noril'sk, which is situated close to the triple junction at the northwestern margin of the Siberian Platform. Presumably these magmas, which have a dominant oceanic island basalt-like asthenospheric mantle geochemical signature, were emplaced during a phase of extension along or close to the Noril'sk-Kharayelakh fault. Subsequently the magmatic activity migrated east and a series of more mafic tholeiites and picritic basalts was emplaced. The strong lithospheric signature of these flows and rapid emplacement in an extensional regime may explain their different compositions compared with the overlying Nadezhdinsky which erupted centred on the Noril'sk-Kharayelakh fault 100 km to the west. Nadezhdinsky lavas contain the largest crustal signature and the strongest chalcophile element depletion and were erupted and emplaced (Naldrett et al. 1992) close to the Noril'sk-Kharayelakh fault. These magmas were presumably derived in part from the lithospheric mantle and the progressive compositional shift may then reflect a systematic change in the proportion of crustal material involved. The variations in chalcophile element abundances would then be consistent with progressive decline in the degree of S saturation as the magmas become progressively less contaminated. The eruption of the Mr-Mk lavas occurred dominantly to the northeast of the Noril'sk District presumably through different fissures, and it is therefore interesting that the magma compositions changed more abruptly as the eruptive fissures relocated.

Acknowledgements. We thank the staff of the Geoscience Laboratories, Ontario Geological Survey and the Isotope Laboratory at the Open University for assistance with analytical work. Dr. V.G. Milne, the Director of the Ontario Geological Survey Geoscience Branch, is thanked for permission for Dr. Peter C. Lightfoot to co-author this paper. We thank the Director of TsNIGRI, Dr. I. Migachev, for access to the material and for permission to publish the data. We acknowledge the great assistance of Academician V. Zharikov, Director of the Institute of Experimental Mineralogy, Russian Academy of Sciences. Reviews by Richard Carlson and Ajoy Baksi were of great assistance in preparing the revised manuscript. Jim Boyd drafted the diagrams and Heidi Hahn typed the manuscript.

References

Campbell IH, Griffiths RW (1990) Implications of mantle plume structure for the evolution of flood basalts. Earth Planet Sci Lett 99:79–93

Cox KG, Hawkesworth CJ (1984) Relative contributions of crust and mantle to flood basalt magmatism, Mahabaleshwar area, Deccan Traps. Phil Trans R Soc London A310:627–641

Cox KG, Hawkesworth CJ (1985) Detailed stratigraphy of the Deccan Traps at Mahabaleshwar, Western Ghats, India, with implications for open system processes. J Petrol 26:355–377

De Paolo DJ, Wasserburg GJ (1976) Inferences about magma sources and mantle structure from variations of $^{143}Nd/^{144}Nd$ Geophys Res Lett 3:743–746

Doherty W (1989) An internal standardization procedure for the determination of yttrium and the rare earth elements in geological materials by inductively coupled plasma-mass spectrometry. Spectrochim Acta 44B:263–280

Doherty W (1991) Developments in geoanalytical inductively coupled plasma mass spectrometry. Ont Geol Surv Misc Pap 157:216–219

Doherty W, Wong P, Hodges AE (1990) Determination of 22 trace elements in geological materials by inductively coupled plasma mass spectrometry. Ont Geol Surv Misc Pap 151:235–238

Ellam R, Cox KG (1991) An interpretation of Karoo continental flood basalts in terms of interaction between asthenospheric magmas and the mantle lithosphere. Earth Planet Sci Lett 105:330–342

Erlank AJ, Duncan AR, Marsh JS, Sweeney RJ, Hawkesworth CJ, Milner SC, Miller RMG, Rogers NW (1988) A laterally extensive geochemical discontinuity in the subcontinental Gondwana lithosphere. In: Abstracts of Conference on geochemical evolution of the continental crust, Vol 1, Brazil, pp 1–10

Fedorenko VA (1979) Paleotectonics of Late Paleozoic-Early Mesozoic volcanism in the Noril'sk region, and paleotectonic controls on the distribution of Ni-bearing intrusions. Geology and ore deposits of Taymeria–Northland Fault Bett. Leningrad, NIIGA 4:16–23

Fedorenko VA (1981) The petrochemical series of volcanic rocks of the Noril'sk region. Geol Geophys 6:78–88

Fedorenko VA (1991) Tectonic control of magmatism and regularities of Ni-bearing localities of the Northwestern Siberian Platform. Geol Geophys 1:48–56

Gallagher K, Hawkesworth CJ (1992) Dehydration melting and the generation of continental flood basalts. Nature 358:57–59

Hawkesworth CJ, Erlank AJ, Marsh JS, Menzies MA, Van Calsteren PWC (1983) Evolution of the continental lithosphere: evidence from volcanics and xenoliths in Southern Africa. In: Hawkesworth CJ, Norry MJ (eds) Continental flood basalts and mantle xenoliths. Shiva, Nantwich, pp 111–138

Hawkesworth CJ, Rogers NW, Van Calsteren PWC, Menzies MA (1984) Mantle enrichment processes. Nature 311:331–335

Hawkesworth CJ, Mantovani MSM, Taylor PN, Palacz Z (1986) Evidence from the Parana of south Brazil for a continental contribution to Dupal basalts. Nature 322:356–359

Hergt JM, Chappell BW, Faure G, Mensing TM (1989a) Geochemical and isotopic constraints on the origin of the Jurassic dolerites of Tasmania. J Petrol 30:841–883

Hergt JM, Chappell BW, McCulloch MT, McDougall I, Chivas AR (1989b) The geochemistry of Jurassic dolerites from Portal Peak, Antarctica. Contrib Mineral Petrol 102:298–305

Hergt JM, Peate DW, Hawkesworth CJ (1991) The petrogenesis of Mesozoic Gondwana low-Ti flood basalts. Earth Planet Sci Lett 105:134–148

Hill RI (1991) Starting plumes and continental break-up. Earth Planet Sci Lett 104:398–416

Krishnamurthy P, Cox KG (1977) Picritic basalts and related lavas from the Deccan Trap of Western India. Contrib Mineral Petrol 73:179–189

Lightfoot PC (1985) Isotope and trace element geochemistry of the South Deccan lavas, India. PhD thesis. Open University UK

Lightfoot PC, Hawkesworth CJ (1988) Origin of the Deccan Trap lavas: evidence from combined trace element and Sr-, Nd-, and Pb-isotope studies. Earth Planet Sci Lett 91:89–104

Lightfoot PC, Hawkesworth CJ, Devey CW, Rogers NW, Van Calsteren PWC (1990a) Source and differentiation of Deccan Trap lavas: implications of geochemical and mineral chemical variations. J Petrol 31-5:1165–1200

Lightfoot PC, Naldrett AJ, Gorbachev NS, Doherty W, Fedorenko VA (1990b) Geochemistry of the Siberian Trap of the Noril'sk area, USSR, with implications for the relative contributions of crust and mantle to flood basalt magmatism. Contrib Mineral Petrol 104:631–644

Lightfoot PC, Chai G, Hodges AE, Rowell D (1991) An update report on the certification of the OGS in-house MRB standard-reference materials. Ont Geol Surv Misc Pap 147:231–236

Morgan WJ (1981) Hotspot tracks and the opening of the Atlantic and Indian Oceans. In: Emiliani C (ed) The sea, Vol 7. Wiley, New York, pp 443–487

Naldrett AJ, Lightfoot PC, Fedorenko V, Doherty W, Gorbachev NS (1992) Geology and geochemistry of intrusions and flood basalts of the Noril'sk Region, USSR, with implications for the origin of the Ni-Cu ores. Econ Geol 87:975–1004

Ontario Geological Survey (1990) The analysis of geological materials, vol II: a manual of methods. Ont Geol Surv Misc Pap 149

Patchett PJ (1980) Thermal effects of basalt on continental crust and crustal contamination of magma. Nature 283:559–561

Pearce JA, Norry MJ (1979) Petrogenetic implications of Ti, Zr, Y, and Nb variations in volcanic rocks. Contrib Mineral Petrol 69:33–47

Potts PJ (1987) A handbook of silicate rock analysis. Blackie, Glasgow

Renne PR, Basu AR (1991) Rapid eruption of the Siberian Traps flood basalts at the Permo-Triassic boundary. Science 253:176–179

Sharma M, Basu AR, Nestorenko GV (1991) Nd-Sr isotopes, petrochemistry, and origin of the Siberian flood basalts, USSR. Geochim Cosmochim Acta 55:1183–1192

Sun SS, McDonough VF (1989) Chemical and isotopic systematics of oceanic basalts: implications for mantle composition and processes. In: Saunders AD, Norry MJ (eds) Magmatism in ocean basins. Geol Soc London Spec Pub 42:313–345

Sun SS, Nesbitt RW, Sharaskin AY (1979) Geochemical characteristics of Mid-Ocean Ridge basalts. Earth Planet Sci Lett 44:119–138

Taylor RT, McLennan SM (1985) In: The continental crust: its composition and evolution. Blackwell, Oxford

Thompson RN, Morrison MA, Dickin AP, Hendry GL (1983) In: Hawkesworth CJ, Norry MJ (eds) Continental basalts and mantle xenoliths. Shiva, Nantwich, pp 158–185

White RS, McKenzie DJ (1989) Magmatism at rift zones: the generation of volcanic continental margins and flood basalts. Geophys Res 94:7685–7730

Zolotukhin VV, Al'mukhamedov AI (1988) Traps of the Siberian Platform In: Macdougall JD (ed) Continental flood basalts. Kluwer Academic Publishers, Dordrecht, pp 273–310

Editorial responsibility: J. Patchett